REPORT DOCUMENTATION PAGE

Form Approved
OMB No. 0704-0188

2. REPORT DATE	3. REPORT TYPE AND DATES COVERED
Summer 1991	THESIS/~~DISSERTATION~~

1

Balanced, Potential Vorticity Dynamics in the Tropics

5. FUNDING NUMBERS

6. AUTHOR(S)

Kenneth W. Harding, Capt

7. PERFORMING ORGANIZATION NAME(S) AND ADDRESS(ES)

AFIT Student Attending: Colorado State University

8. PERFORMING ORGANIZATION REPORT NUMBER

AFIT/CI/CIA- 91-105

9. SPONSORING/MONITORING AGENCY NAME(S) AND ADDRESS(ES)

AFIT/CI
Wright-Patterson AFB OH 45433-6583

10. SPONSORING/MONITORING AGENCY REPORT NUMBER

11. SUPPLEMENTARY NOTES

12a. DISTRIBUTION/AVAILABILITY STATEMENT

Approved for Public Release IAW 190-1
Distributed Unlimited
ERNEST A. HAYGOOD, Captain, USAF
Executive Officer

12b. DISTRIBUTION CODE

13. ABSTRACT (*Maximum 200 words*)

14. SUBJECT TERMS

15. NUMBER OF PAGES
75

16. PRICE CODE

17. SECURITY CLASSIFICATION OF REPORT	18. SECURITY CLASSIFICATION OF THIS PAGE	19. SECURITY CLASSIFICATION OF ABSTRACT	20. LIMITATION OF ABSTRACT

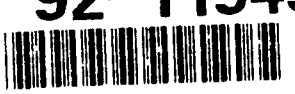

THESIS

BALANCED, POTENTIAL VORTICITY DYNAMICS IN THE TROPICS

Submitted by

Kenneth W. Harding

Department of Atmospheric Science

In partial fulfillment of the requirements

for the degree of Master of Science

Colorado State University

Fort Collins, Colorado

Summer, 1991

COLORADO STATE UNIVERSITY

April 16, 1991

WE HEREBY RECOMMEND THAT THE THESIS PREPARED UNDER OUR SUPERVISION BY KENNETH W. HARDING ENTITLED BALANCED, POTENTIAL VORTICITY DYNAMICS IN THE TROPICS BE ACCEPTED AS FULFILLING IN PART REQUIREMENTS FOR THE DEGREE OF MASTER OF SCIENCE.

Committee on Graduate Work

David A. Randall

Paul J. Mielke

Wayne Schubert

Co-adviser

Duane E. Stevens

Co-adviser

Stephen K. Cox

Department Head

ABSTRACT OF THESIS

BALANCED, POTENTIAL VORTICITY DYNAMICS IN THE TROPICS

A scheme for describing tropical atmospheric flow is analyzed. Based on the quasi-balanced approximation from Stevens *et al.* (1990), attempts are made to test the validity of the approximation. Isentropic potential vorticity, being a critical variable in the approximation, is calculated using data gathered during Phase II of the Australian Meteorological Experiment (AMEX). These isentropic potential vorticity fields are then examined in terms of the Charney-Stern theorem for instability. It is found that there is a consistent area of reversed equator-to-pole gradient of potential vorticity. This area is susceptible to combined barotropic-baroclinic instability.

After reviewing several previous attempts to quantify tropical atmospheric flow, the quasi-balanced approximation from Stevens *et al.* (1990) is tested using archived data for several different time frames and levels in the atmosphere. It is found that the quasi-balanced approximation works very well for areas not dominated by convection. In these convective areas, however, there appears to be a weakness in the approximation.

Kenneth W. Harding
Department of Atmospheric Science
Colorado State University
Fort Collins, Colorado 80523
Summer, 1991

ACKNOWLEDGEMENTS

I would like to extend both my thanks and admiration to my advisor, Dr. Wayne Schubert. He has proven to be a great inspiration both in and out of class, and his teaching ability is second to none. Thanks also to Dr. David Randall, Dr. Duane Stevens, and Dr. Paul Mielke for their many helpful suggestions. I would also like to thank Paul Ciesielski for his countless hours helping me with my many new and unique computer problems. Thank you, Gail Cordova, for helping prepare this manuscript. I also want to thank the United States Air Force for allowing me to continue my education. Lastly, I want to thank my wife, Denise. She has endured many long days, late nights, and disappearing weekends. I couldn't have done it without her.

This research was supported by NSF grants ATM 83860971 and ATM 8814541. Computing resources were provided by the National Center for Atmospheric Research, which is sponsored by the National Science Foundation.

TABLE OF CONTENTS

LIST OF FIGURES

Chapter 1

INTRODUCTION

Improved atmospheric predictability is one of the main goals of atmospheric research, and uncounted hours have been spent on this problem. Historically, beginning even before Rossby, much attention has been given to the middle latitudes. With the rise of global modelling and satellite data, however, there is now also considerable interest in the tropical atmosphere.

One early attempt to provide a predictability scheme for the tropics was done by Matsuno in 1966. He tried to use middle latitude-based, quasi-geostrophic theory to describe important features of tropical motions. His results were disappointing. Besides not being able to describe the mixed Rossby-gravity wave, the quasi-geostrophic method completely neglected the equatorially trapped Kelvin wave. This Kelvin wave has been implicated in many important tropical flow features, including the Quasi-Biennieal Oscillation (QBO). Several attempts have been made since Matsuno, and the basis for calculations presented herein is one of those attempts.

Stevens *et al.* (1990) presented a system of equations they called the quasi-balanced approximation. This scheme includes the important Kelvin waves, and has appropriate energy conservation relationships. While the mathematics are indeed eloquent, the following question arises: Is the approximation, based on the neglect of meridional acceleration in the meridional momentum equation, valid? This thesis tries to answer this question in several different ways.

In 1985, Hoskins *et al.* stressed the importance of "potential vorticity thinking" . This variable is important because it contains information on both dynamics and thermodynamics, and is conserved for frictionless, adiabatic motion. Thus, potential vorticity is

very useful as a tracer for the flow. Schubert *et al.* (1991) also stressed the importance of potential vorticity dynamics as a possible way to unite the middle latitudes and tropical atmospheres into one system of predictability equations. The proposed approximation of Stevens *et al.* is only quasi-balanced because if the variable of potential vorticity is inverted, no information about the Kelvin wave is included, as Kelvin waves are motions that have zero potential vorticity. Thus, if this approximation is ever expanded to be a basis for prediction, some other variable (such as angular momentum) should be the primary predicted variable.

The outline of this paper is as follows. Chapter two, based on the importance of potential vorticity, presents calculations of isentropic potential vorticity. Calculations were made using the data gathered during the Australian Meteorological Experiment (AMEX). Chapter three is a review of several attempts to quantify tropical motions, concluding with the recent work of Stevens *et al.* (1990). Chapter four is a test of the quasi-balanced approximation using historical data. Different time frames are examined, including a 'normal' time (January 1981), and a large departure from the normal state of the tropical atmosphere (January 1983). The quasi-balanced approximation is tested both by calculation of potential vorticity and calculation of terms in the meridional momentum equation. These calculated fields are then compared to actual fields, as in the case of potential vorticity, or compared to the theoretically perfect balance, as in the case of the meridional momentum equation. Chapter five presents our conclusions.

Chapter 2

POTENTIAL VORTICITY ANALYSIS AND MODELING OF THE HADLEY CIRCULATION

The use of potential vorticity as a meteorological tracer to more easily understand dynamical processes was highlighted by Hoskins *et al.* (1985), although the concept of potential vorticity was introduced in 1940 by Rossby. Potential vorticity is conserved for adiabatic, frictionless motion. The concept of potential vorticity is quite simple. There is a potential for 'creating' vorticity (positive or negative) by changing latitude and/or by adiabatically changing the separation of isentropic layers (Hoskins *et al.*, 1985). The simple form of the conservation relationship as envisioned by Rossby was

$$\frac{\zeta_a}{h} = \text{constant} , \tag{2.1}$$

where h is the depth of the fluid in a barotropic model and ζ_a is the absolute (earth's plus relative) vorticity. This idea was extended to an isentropic coordinate system yielding

$$P_r = \left(\frac{f + \zeta_\theta}{D} \right) , \tag{2.2}$$

where f is the coriolis parameter, $D = -\delta p/g$ is the mass per unit area, and $\zeta_\theta = (\partial v/\partial x)_\theta - (\partial u/\partial y)_\theta$ is the isentropic vorticity. Ertel (1942), in independent research, gave the result in Eq. (2.1) full hydrodynamical generality by allowing adiabatic motion, and thus derived the following:

$$P = \frac{1}{\rho} \zeta_a \cdot \nabla\theta = \text{constant} . \tag{2.3}$$

The beauty of potential vorticity as defined by Ertel in Eq. (2.3) is that no approximations (such as the hydrostatic approximation) are made. Equation (2.3) is valid for three

dimensional, nonhydrostatic motions. By combining both mass and thermodynamics, Eq. (2.3) shows another value of potential vorticity. Once potential vorticity is known, the wind and pressure fields can be recovered by inverting the potential vorticity fields as done by Hoskins *et al.*, (1985).

While the above is useful, it is not the frictionless, adiabatic motions that are of interest here. In the Inter Tropical Convergence Zone (ITCZ), strong convective release of latent heat and loss of mass in the form of precipitation from the air parcels causes potential vorticity to be non-conservative.

We can rewrite Eq. (2.3) as

$$\frac{dP}{dt} = \frac{1}{\rho}(\zeta_a \cdot \nabla Q) \ . \tag{2.4}$$

This form of potential vorticity neglects friction. Q represents a heating source. By making the hydrostatic approximation to Eq. (2.4), it becomes

$$\frac{dP}{dt} = -g\left[\zeta_a\left(\frac{\partial Q}{\partial p}\right) + \frac{\partial u}{\partial p}\left(\frac{\partial Q}{\partial y}\right)_p\right] \ , \tag{2.5}$$

where g is the gravitational constant (9.81 ms^{-2}). Assuming a standard profile of heating due to the release of latent heat in the tropical atmosphere, i.e., setting the level of maximum heating to about 500 mb (Yanai *et al.* 1973), in the low levels, $\partial Q/\partial p$ is negative and invokes a concentration of positive potential vorticity, and a concentration of negative potential vorticity aloft (above the height of maximum heating). It is this convective concentration of potential vorticity that will be explored in greater detail.

2.1 Necessary Condition for Instability

Atmospheric flow in the tropics can be shown to be quite different than mid-latitude flow. Temperature advection, critically important in mid-latitudes, is negligible in the tropics over large areas. Thus, in the absence of precipitation, vertical motion in the tropics is very small. This allows us to use the barotropic vorticity equation to approximate large scale motions in the tropics.

$$\left(\frac{\partial}{\partial t} + \boldsymbol{v} \cdot \nabla\right)(\zeta + f) = 0 \tag{2.6}$$

where ζ is the relative vorticity. An important relationship can be derived from Eq. (2.6). If one takes Eq.(2.6), linearizes about a zonal flow dependent only on latitude, and assumes wave-type solutions, after several steps, the following results. In order for a disturbance to convert potential energy of the mean flow into kinetic energy of a perturbation (i.e. to grow), the following condition must be met:

$$\beta - \frac{d^2\bar{u}}{dy^2} = 0 \ , \tag{2.7}$$

where $\beta = \partial f/\partial y$ and $\bar{u}$ = mean zonal velocity. The condition stated in Eq. (2.7) implies that the gradient of absolute vorticity must change sign somewhere in the flow. It is in these areas of a reversed gradient of absolute vorticity that barotropic perturbations are able to grow. Note that the barotropic consequences require absolute vorticity to change sign. We could just as easily have used potential vorticity. In fact, when one uses barotropic-type arguments, the potential vorticity reduces to the absolute vorticity. Thus the necessary (but not sufficient) condition for barotropic instability (Eq. 2.7) is also valid for potential vorticity.

2.2 Burpee (1972) Review

The study of west African waves undertaken by Burpee in 1972 revealed many of their characteristics. West African waves are clearly important, accounting for about half of the tropical cyclones in the Atlantic every year (Frank, 1970). Burpee made an attempt to understand the physics of wave generation. His 1972 paper stressed the importance of the Sahara Desert surface temperatures, noting that the mean surface temperature changes by 10.0 degrees C. in 10 degrees latitude. This strong, reversed equator to pole temperature gradient was theorized by Burpee to cause the thermal wind to blow strongly from the east. Indeed, there is a strong easterly jet appearing at approximately 700 mb. This jet is maintained by a thermally direct, ageostrophic circulation. This circulation acts as a source of kinetic energy for the jet, and the thermally direct circulation is maintained

by the strong surface temperature gradient in the Sahara Desert area. Once the easterly jet is established by the surface temperature gradient, Burpee invoked the Charney-Stern theorem for an internal jet. This jet, being unstable, was able to provide energy to the growing disturbances. Burpee even showed that there was an area of reversed potential vorticity gradient where the waves appeared to form. His entire physical explanation of these African waves was based on the surface temperature gradient south of the desert region. In his final statement, he writes "The role of convection in these disturbances has so far not been conclusively determined, and the limited north-south extent of surface and rawinsonde observations precludes the possibility of investigating whether the ITCZ is directly involved with these waves". This is a possibility that needs exploring. Can areas of reversed potential vorticity gradient be found in other tropical latitudes with easterly jets and convective forcing? Schubert *et al.* (1991) modelled the potential vorticity generation by ITCZ convection in the Hadley cell. They found that the convection alone can cause a reversal in the gradient of potential vorticity on the time scale of about 5 days. This gradient reversal manifests itself without invoking any surface heating to the poleward side of the ITCZ. The same model that was used in Schubert *et al.* (1910) was used in this study, with the results appearing in a later section of this paper.

2.3 Potential Vorticity Calculations

If the arguments in the previous section are correct, the following quote from Schubert *et al.* (1991) needs to be considered... "From the model simulations it is clear that the instability of the lower tropospheric easterly jet can be explained by ITCZ convection alone; there is no reason to invoke surface heating in the Saharan region. Once this is accepted, there is no reason to regard the African region as particularly unique, and we should expect this same instability and breakdown of the easterly jet in all regions with a well defined ITCZ." Schubert notes two regions of possible interest; the northern Australian area and the tropical east Pacific.

We will concentrate on the northern Australian area as the amount of data, both upper air and surface, is greater. Another consideration that made this region more

attractive was the Australian Monsoon Experiment (AMEX). AMEX was a two part experiment held between October 1986 and February 1987. Special observation sites were added to the northern Australian area to collect concentrated data. Collection methods included rawinsondes, radars, ship observations, and research aircraft flights. AMEX had the purpose of investigating the interactions between cumulonimbus convection and the Australian summer monsoon circulation (Gunn *et al.*, 1989). The data set produced from this experiment is impressive. It is contained in a domain from 110 degrees east to 155 degrees east, and from the equator to 30 degrees south. This data set, with a horizontal resolution of 1.5 degrees, was used to calculate potential vorticity over the AMEX domain. Both horizontal plots, to show spatial structure, and vertical cross sections were produced. The goal was to produce maps similar to those presented by Burpee in 1972, which showed an area of reversed pole to equator potential vorticity gradient to be a long term condition.

2.3.1 AMEX data

While the AMEX Phase II (10 January to 15 February 1987) was ongoing, there was an onset of the summer monsoon, a period of active convection and two tropical cyclones, a 'break' in the monsoon, and a resumption of the monsoon flow. We would like to present plots from the 'break' period and from an active period. Gunn *et al.* (1989) described these periods in detail, and the choice of active vs. inactive was chosen based on their analyses. The active period used was 1–3 February 1987, while the inactive period was 25–27 January, 1987. Figures 2.1 and 2.2 show satellite pictures of the Australian area for these two periods. The difference in the amount of convection is readily visible. In the active case (Fig. 2.1), there is a significant amount of organized convection present; organization which is lacking in the inactive case (Fig. 2.2).

Figures 2.3 a–b show the zonal wind fields at 850 mb. What is very obvious is that the active period, shown in Fig. 2.3a, has much stronger westerly flow near 10 degrees south, and the easterly flow south of the monsoon trough is stronger and more organized. Davidson *et al.* (1984) showed that the weakening of the westerlies corresponded to the weakening of the entire monsoon circulation, and this is just what is seen in Figs. 2.3 a–b.

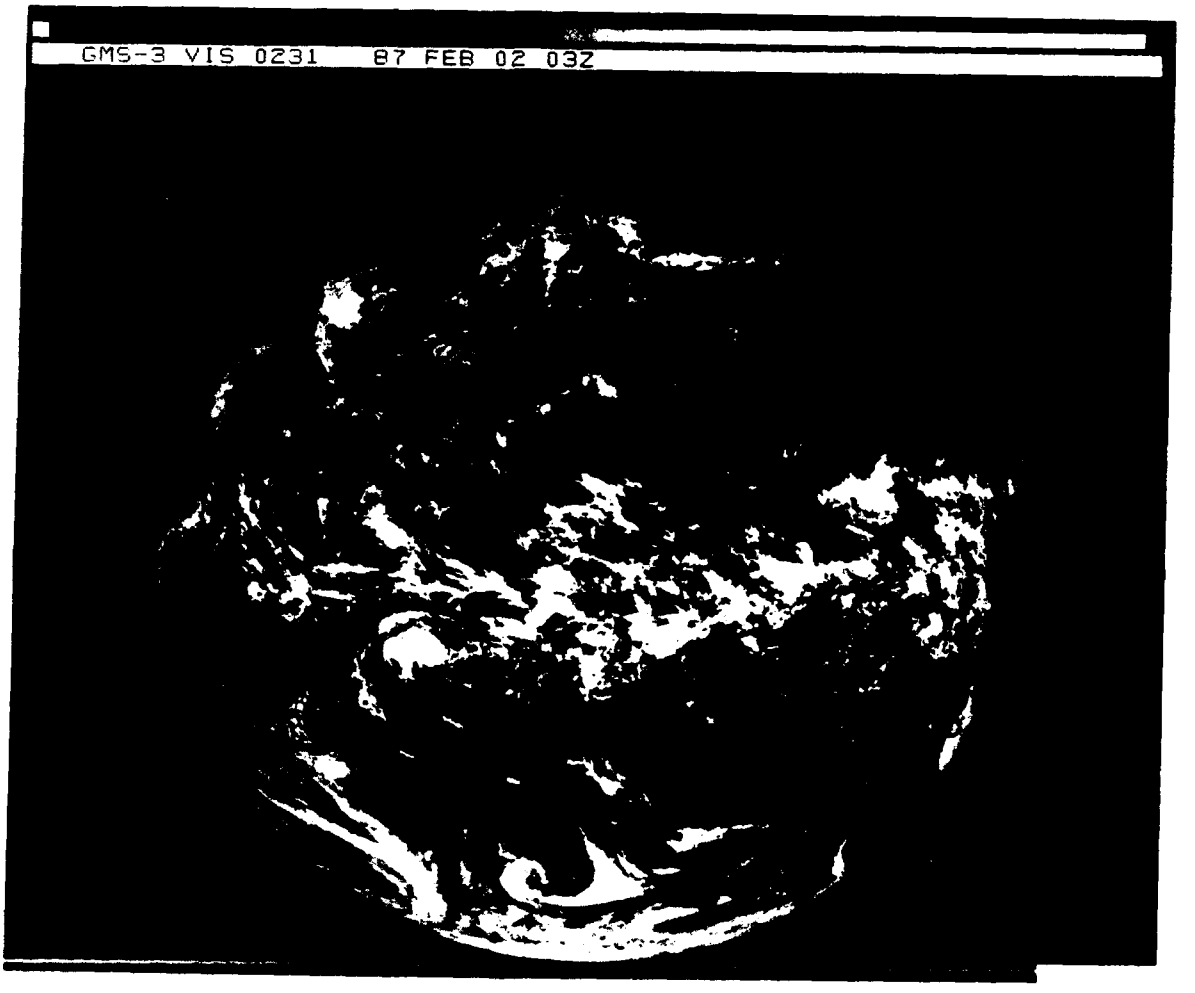

Figure 2.1: GMS visible satellite image from 02 February, 1987, 03Z.

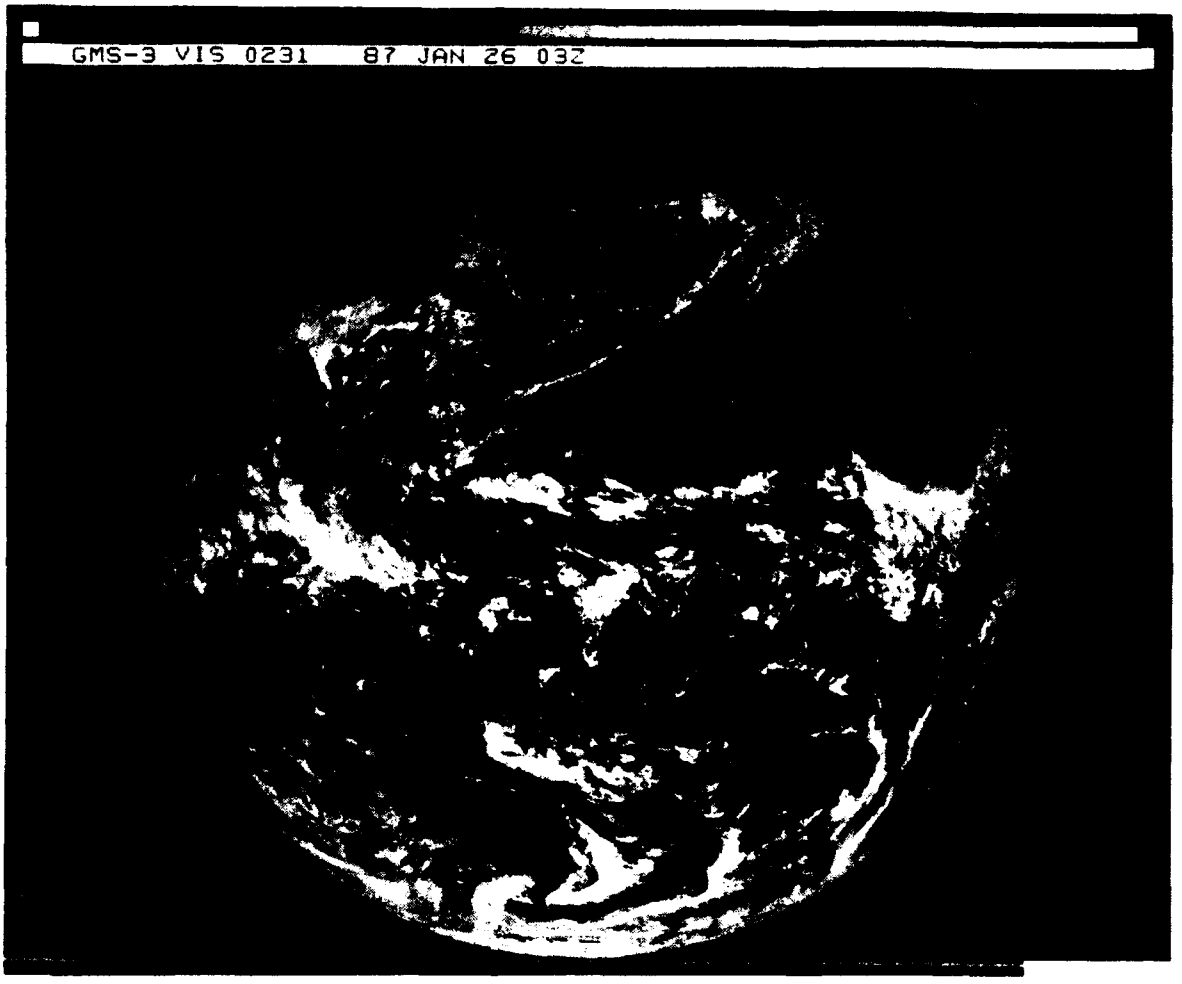

Figure 2.2: GMS visible satellite image from 26 January, 1987, 03Z.

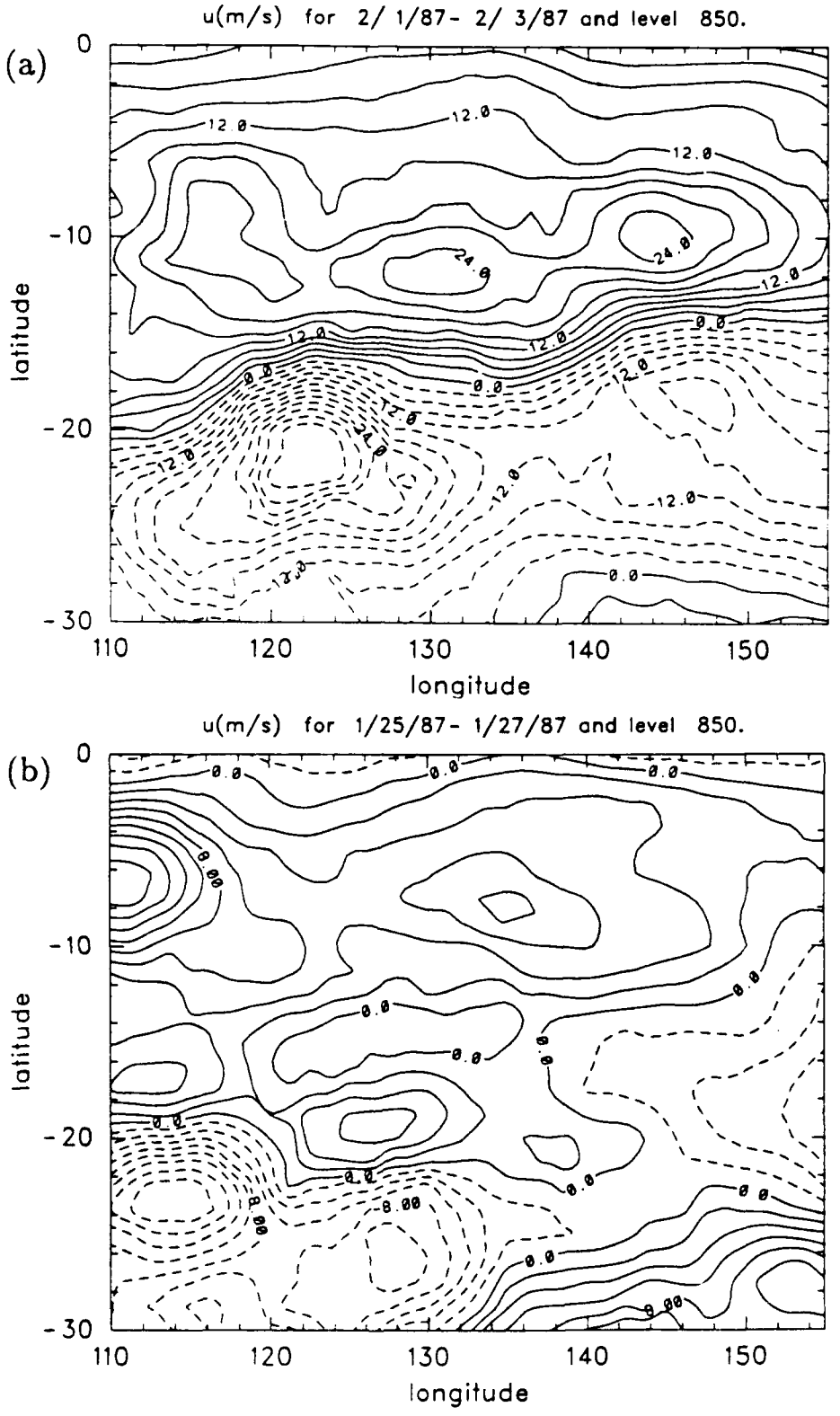

Figure 2.3: Zonal wind field at 850 mb for (a) 2/1/87 – 2/3/87 and (b) 1/25/87 – 1/27/87. Units are ms^{-1}

Note also that the flow at 850 mb has values that go as high as 36 ms^{-1} in the active case. This is quite strong flow.

Figures 2.4 a–b show the zonal wind fields at 500 mb. Again, note the more organized structure and the higher relative values in the active (Fig. 2.4a) vs. the inactive (Fig. 2.4b). Figures 2.5 a–b show the potential vorticity field at 500 mb. The field has been normalized by a factor proportional to $2\Omega\sigma$, where σ is a reference stability. This was done so that the plots are dimensionless and are compatible with those of the modelled potential vorticity fields presented later in this paper. Several things stand out in this figure. In 2.5a, the active case, there is a strong relative minimum value of potential vorticity located near 15 degrees south and 120 degrees east. Poleward of this area, the necessary condition for combined barotropic-baroclinic instability is met. While this condition is also met several other places in both figures, this is definitely the strongest gradient reversal area.

Figures 2.6 a–b show the potential temperature field for both periods. These fields appear nearly identical. The relative maximum value south of 20 degrees south is due to the high surface temperatures over the Australian landmass. Note how uniform the upper level isentropes are. When looking for a reversal in the gradient of potential vorticity, it is along these isentropes that the gradient must be examined. With these isentropic surfaces being nearly parallel to the pressure surfaces, it will be easy to visualize the areas of reversed gradient.

Figures 2.7 a–b show the zonal wind for the two periods. Again, notice how the westerly flow has weakened to a point where it is almost nonexistent during the inactive period. The easterly flow has also weakened considerably, and westerlies have invaded the southern part of the domain.

Finally, Figs. 2.8 a–b are presented. These cross sections are taken at 140 degrees east longitude. The main feature in Fig. 2.8a is the strong relative minimum potential vorticity values near the center of the plot. Just poleward of this area, the necessary condition for combined barotropic-baroclinic instability is met. The areas of positive potential vorticity near the surface in Fig 2.8b are due to the rapidly decreasing temperature above the surface. This rapidly decreasing temperature causes the vertical derivative of potential

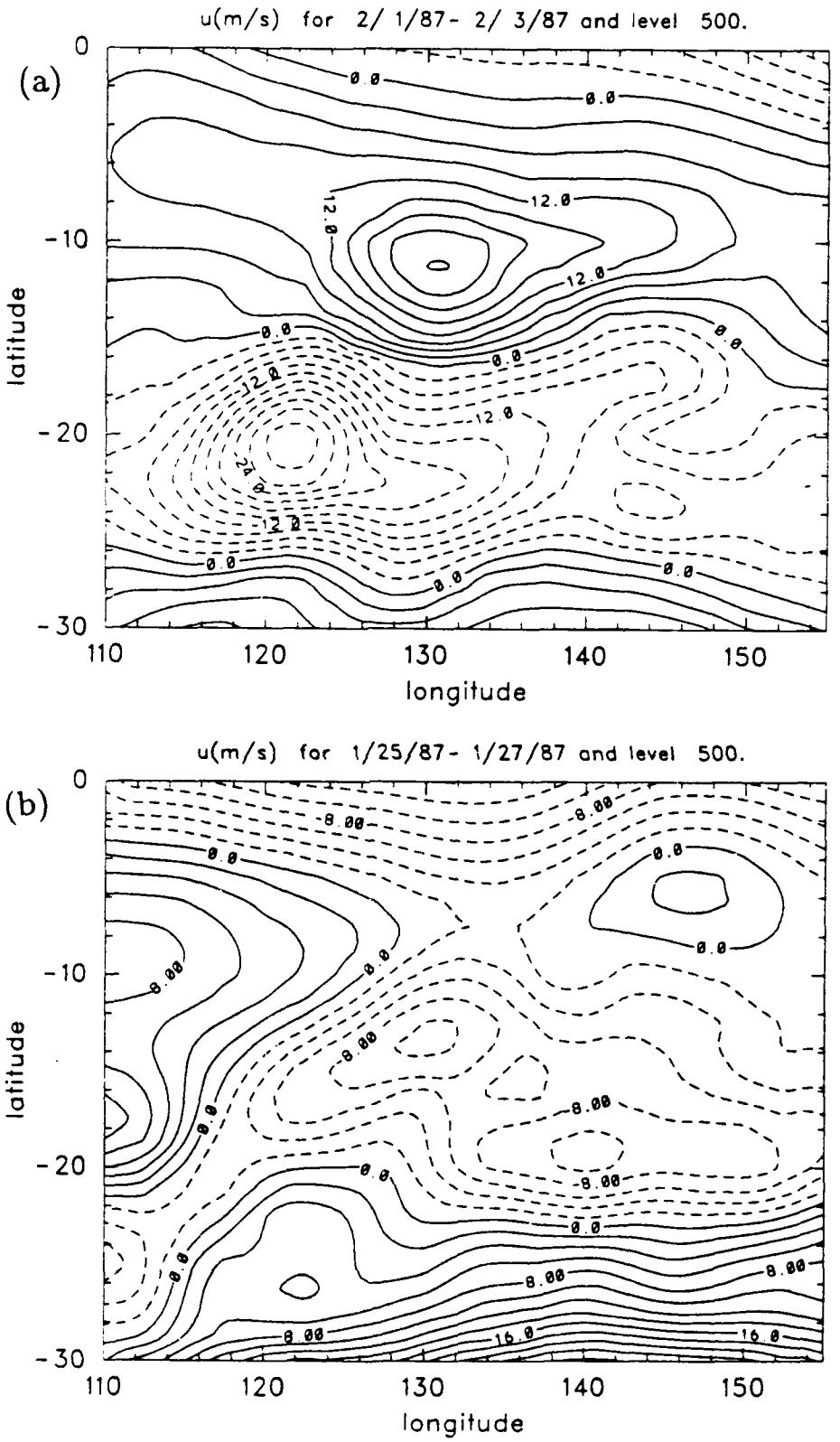

Figure 2.4: As in Fig. 2.3 except for 500 mb and (a) 2/1/87 - 2/3/87 and (b) 1/25/87 - 1/27/87.

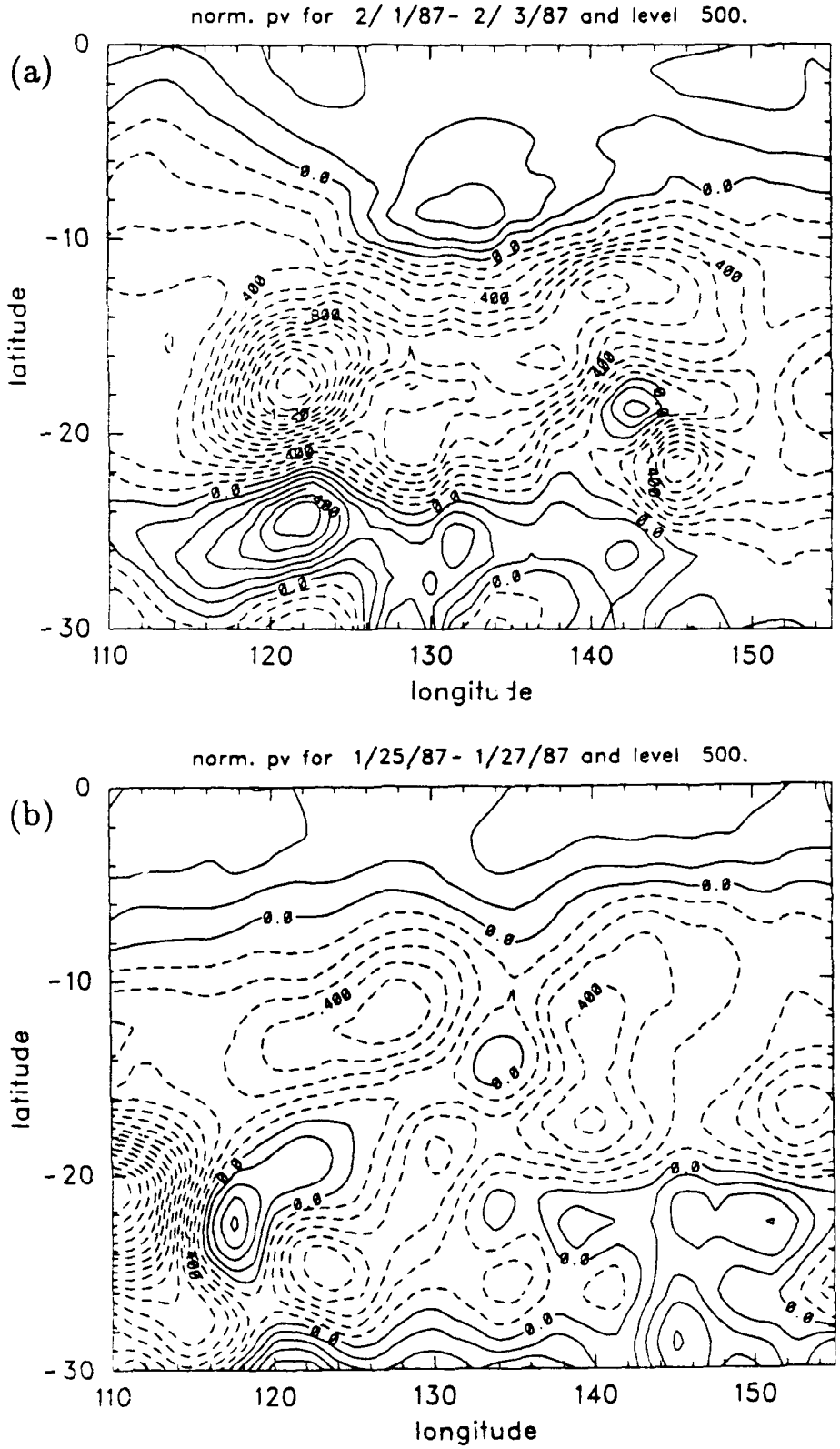

Figure 2.5: Normalized potential vorticity at 500 mb for (a) 2/1/87 - 2/3/87 and (b) 1/25/87 - 1/27/87.

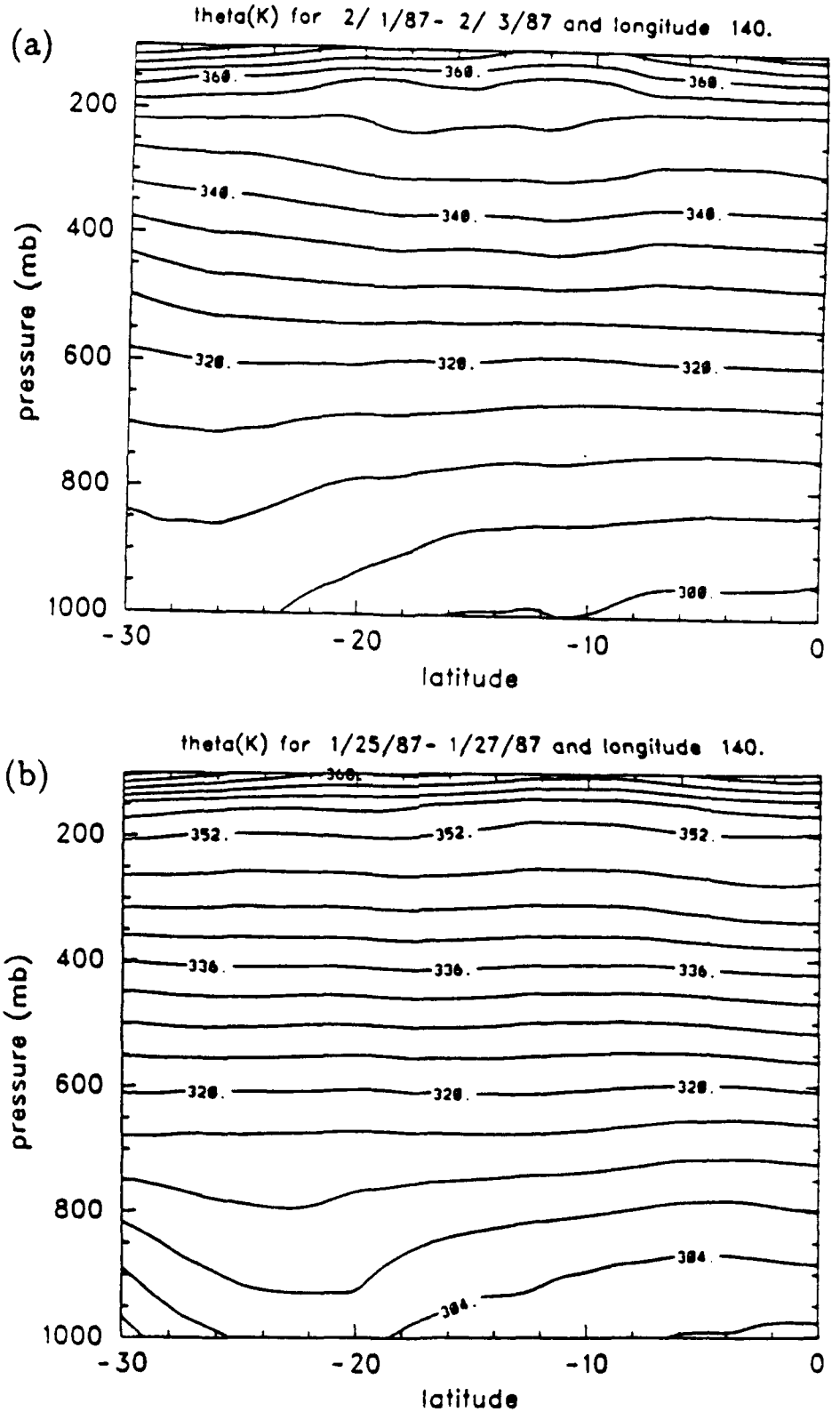

Figure 2.6: Cross section plots at 140 degrees east of potential temperature for (a) 2/1/87 -2/3/87 and (b) 1/25/87 - 1/27/87. Units are degrees Kelvin.

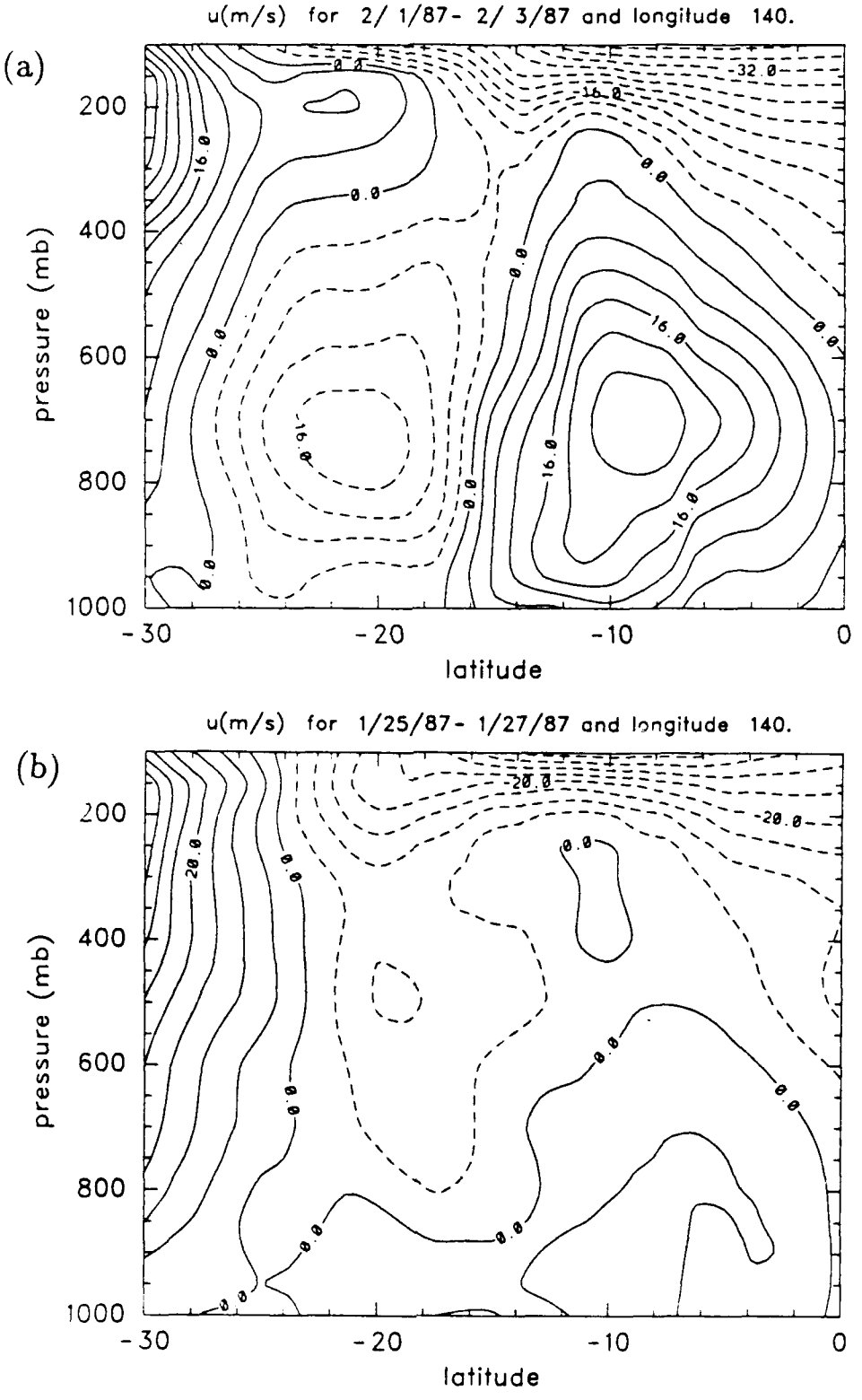

Figure 2.7: Cross section plots at 140 degrees east of zonal winds for (a) 2/1/87 - 2/3/87 and (b) 1/25/87 - 1/27/87. Units are ms^{-1}.

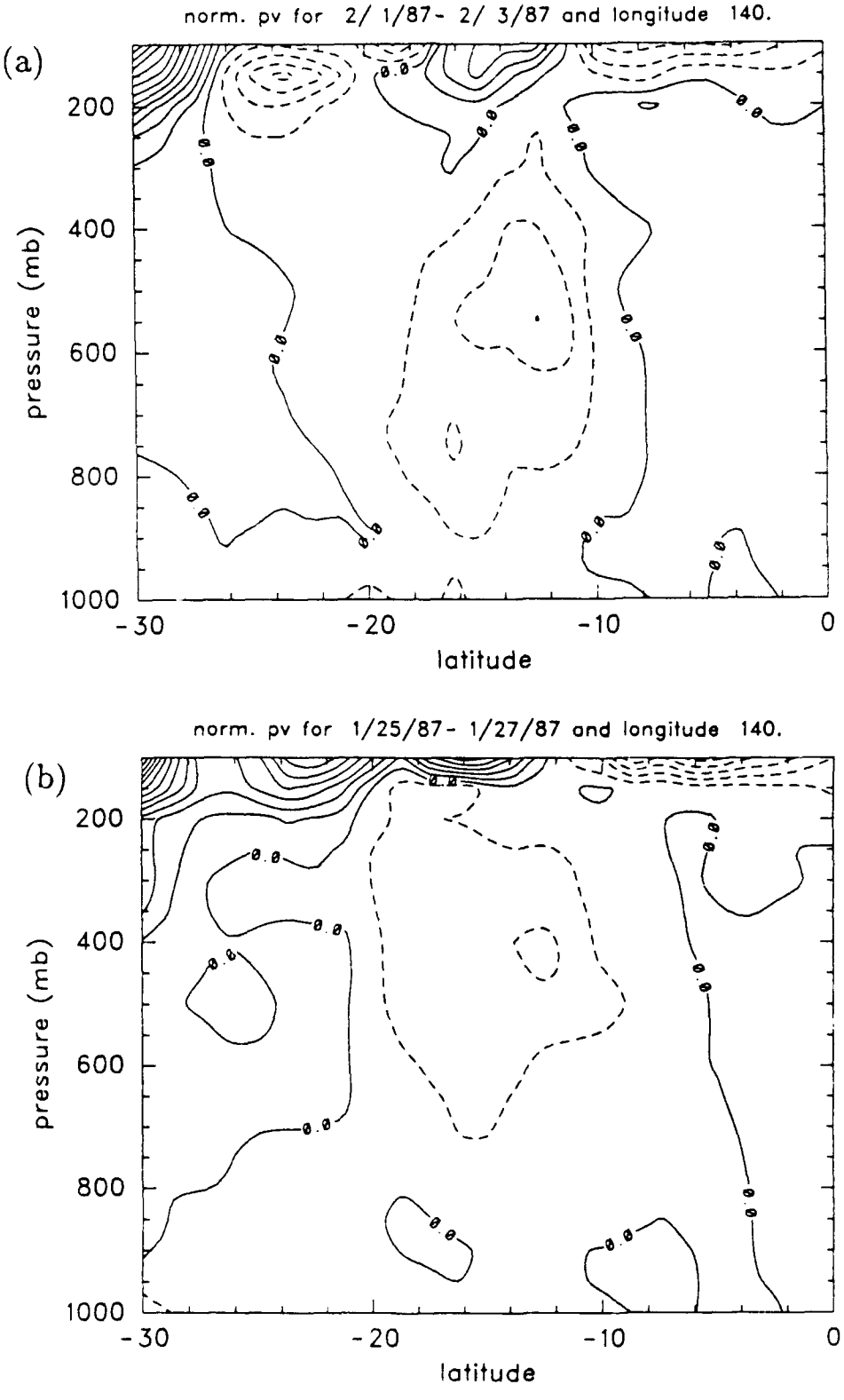

Figure 2.8: Cross section plots at 140 degrees east of normalized potential vorticity for (a) 2/1/87 - 2/3/87 and (b) 1/25/87 - 1/27/87.

temperature to dominate, and as the cooling decreases, it changes the sign of the potential vorticity, thus causing a positive area of potential vorticity to appear. The negative area above and equator ward of the main area of gradient reversal was explained by Schubert *et al.* (1991). They theorized that this area of negative potential vorticity is advected there by the top portion of the Hadley circulation. While the area of relative minimum potential vorticity is much less significant in the inactive (Fig. 2.8b) case, there is still a hint of gradient reversal.

Figures 2.9 a–b now take the entire AMEX domain, and sector average. Notice that over the entire experiment area, there is a vast difference in the wind field for active vs. inactive periods. The changes, for such a short time and large area, are dramatic indeed.

Equally impressive are Figs. 2.10 a–b. The sector averaged potential vorticity fields appear quite different. During the active period of the monsoon, (Fig. 2.10a), convection is widespread and strong. This convection causes a concentration of negative potential vorticity near the monsoon trough. This relative minimum value of potential vorticity thus upsets the expected pole-to-equator gradient of potential vorticity, causing an area of reversed gradient. In this area, the necessary condition for combined barotropic-baroclinic instability is met. Again, even in the inactive period, there is a hint of an area of gradient reversal.

Figures 2.11 a–b are for a longer time period. The time from 1 February to 15 February 1987 was characterized as active by Gunn *et al.* (1989). The potential temperature field appears quite uniform, while the zonal winds show a robust circulation ongoing for this 15 day period. Figure 2.12 shows the sector averaged potential vorticity for this time period. This field is very consistent with the previous plots of potential vorticity during active periods of the monsoon. This is a remarkable figure, however, when one realizes that this is for a large domain, and for 15 days. For an instability-prone area to exist for such a long time, without being destroyed by instabilities, is interesting. This figure corresponds well to the one month average potential vorticity field shown by Burpee in 1972. While Burpee was concerned with Africa, he suggested that the surface temperatures were the cause of the potential vorticity anomaly. The preceding calculations have

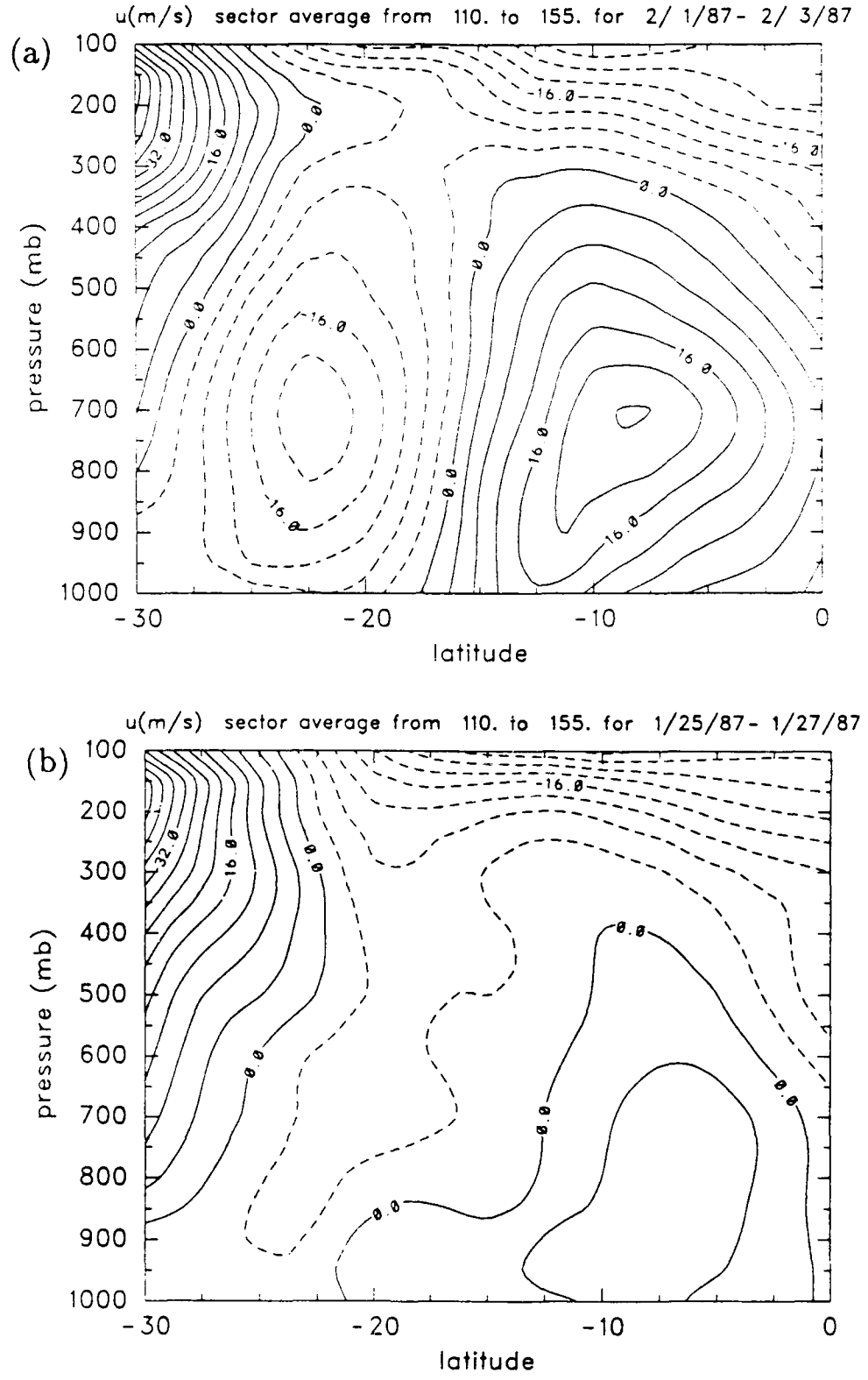

Figure 2.9: Sector averaged cross section of zonal wind for (a) 2/1/87 - 2/3/87 and (b) 1/25/87 - 1/27/87. Units are ms^{-1}.

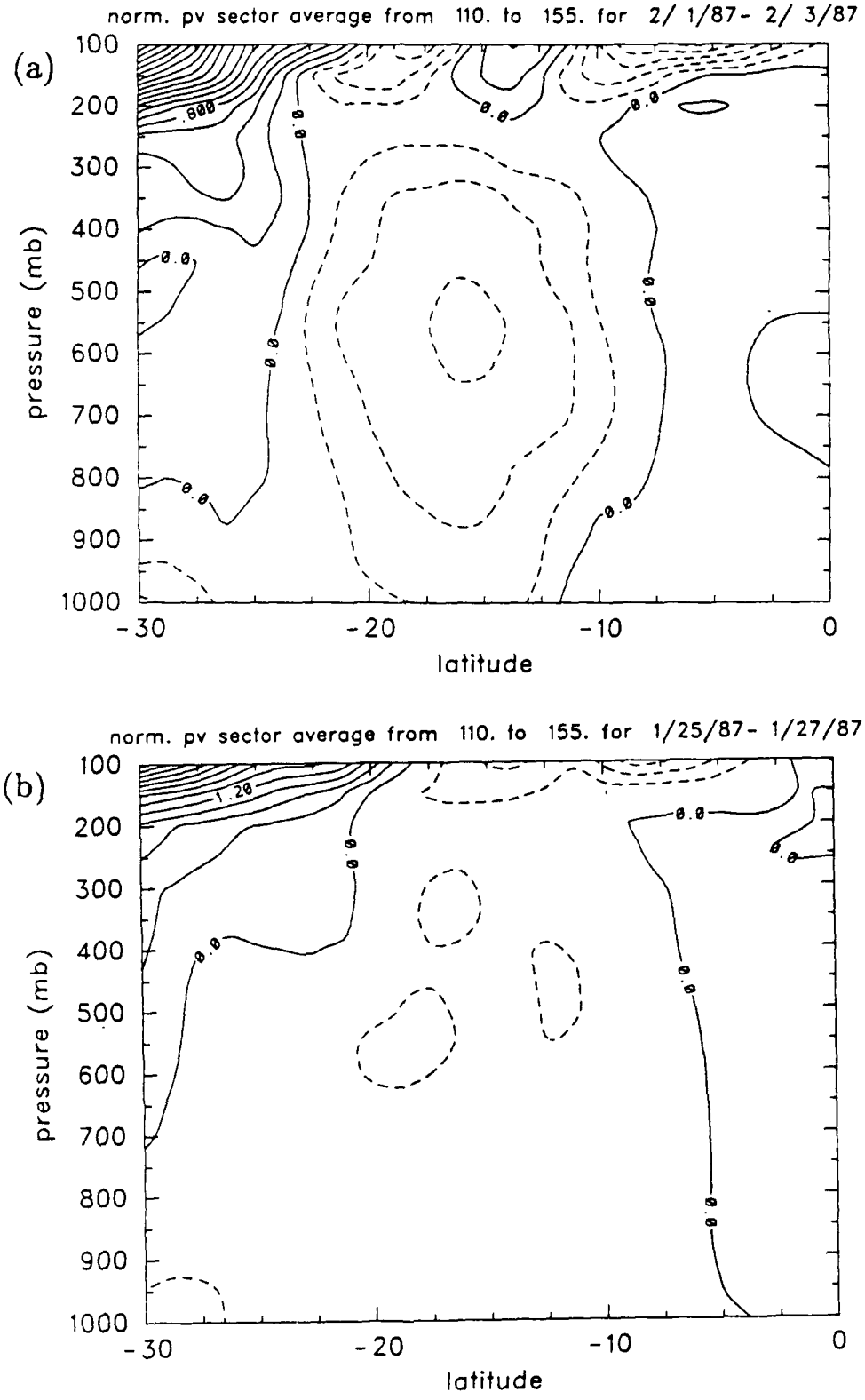

Figure 2.10: Sector averaged cross section of normalized potential vorticity for (a)2/1/87 - 2/3/87 and (b) 1/25/87 - 1/27/87.

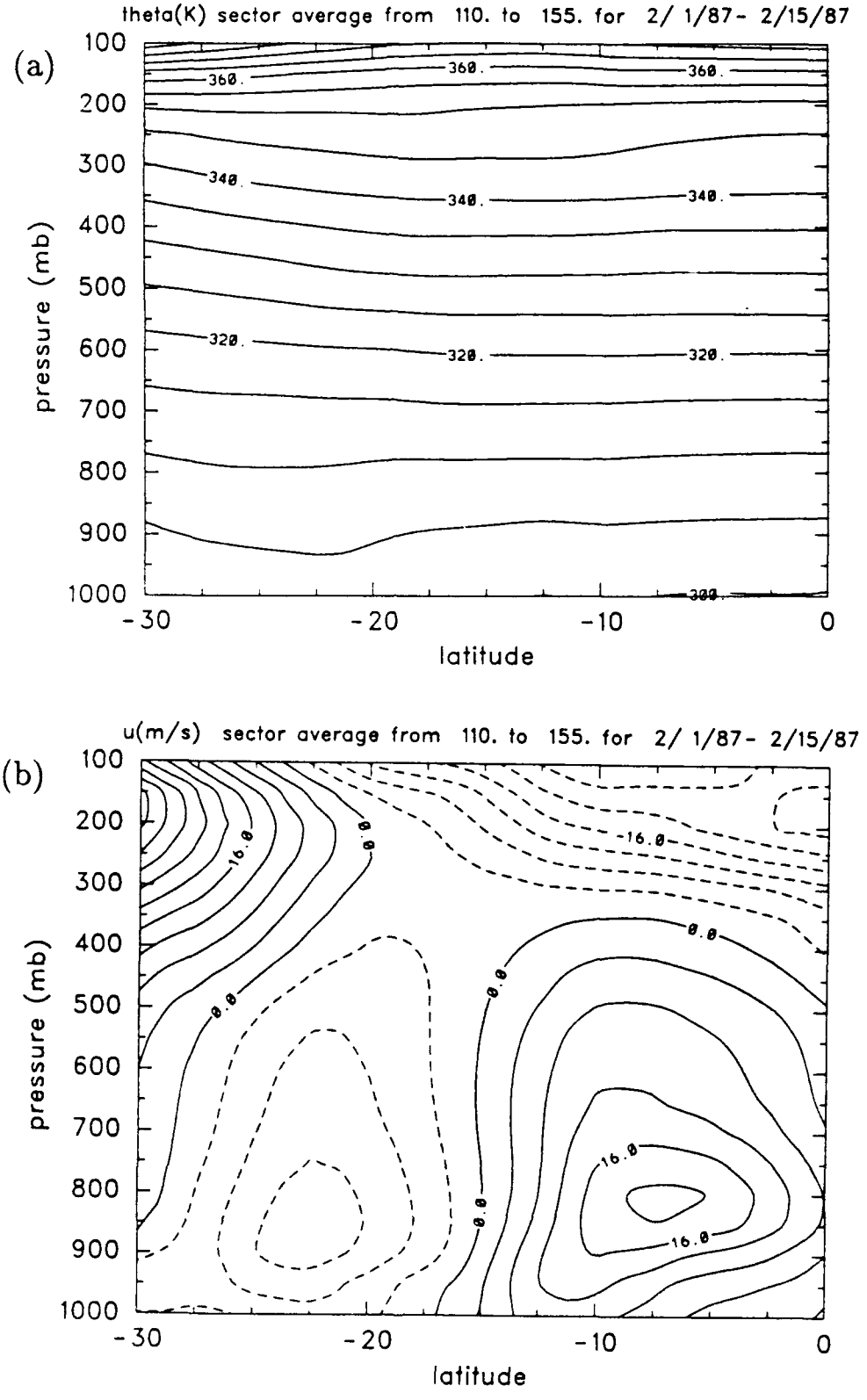

Figure 2.11: Sector averaged cross section for 2/1/87 – 2/15/87 of (a) potential temperature (degrees Kelvin) and (b) zonal wind (ms^{-1}).

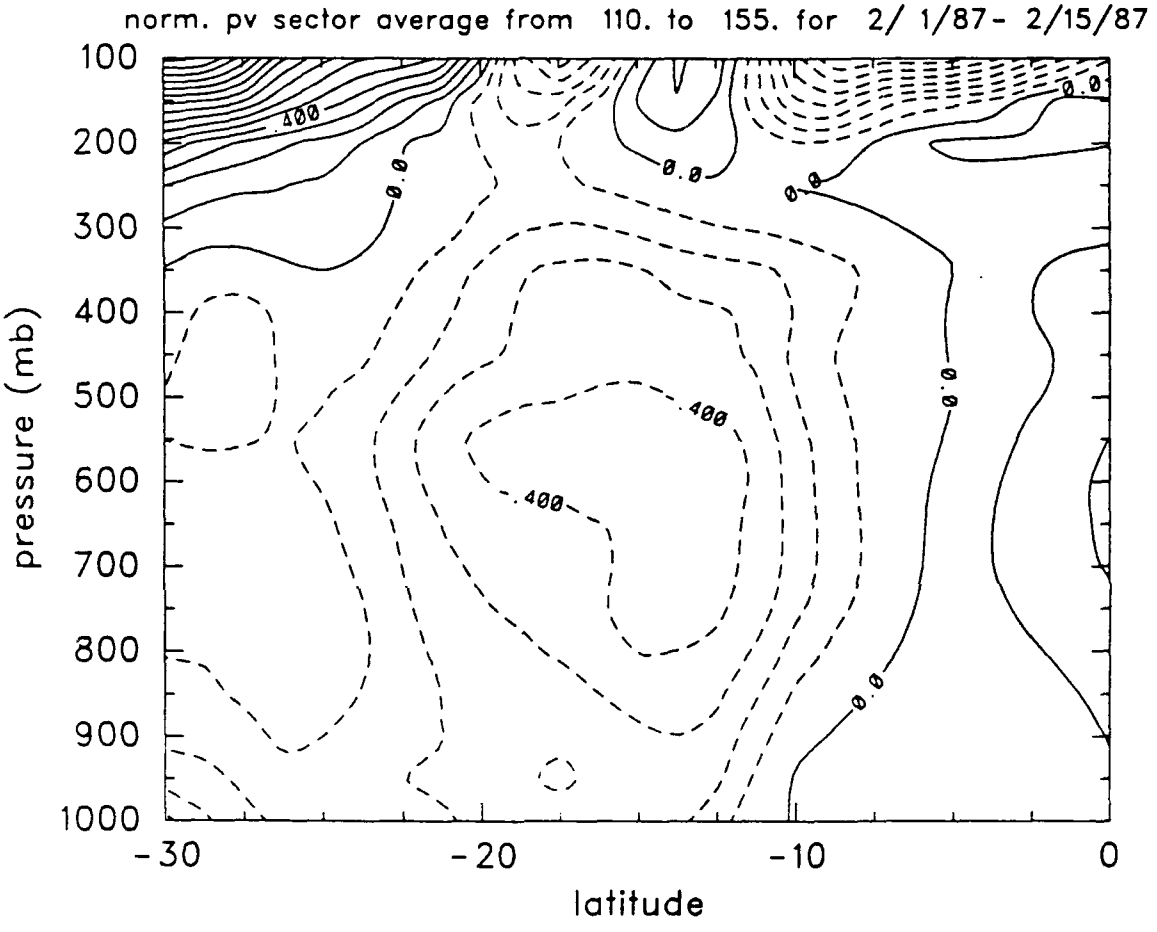

Figure 2.12: Sector averaged cross section for 2/1/87 – 2/15/87 of normalized potential vorticity

shown that the area of Africa is not unique . It is possible, even probable. that areas of reversed potential vorticity gradient can be formed by convective forcing alone, without ever invoking surface heating as a required process.

2.3.2 NMC DATA

While the AMEX data set is impressive in its resolution, there is no information contained for the winter (northern) hemisphere. Even though all of the 'action' is in the summer hemisphere, there are still important physical processes occurring in the northern hemisphere. Schubert *et al.* (1991) note that the generation of winds in the hemisphere opposite that of the main convection can be important. It is for this reason that calculations will be presented that now include the northern hemisphere.

The data set used for the following calculations is National Meteorological Center (NMC) archived gridpoint data with a resolution of 2.5 degrees. Figure 2.13 shows the 850 mb zonal wind field for the active portion of the monsoon. Visible is the broad area of strong westerlies in the monsoon trough vicinity. One important feature of this plot is that when compared to Fig. 2.3a, the AMEX derived zonal winds, the NMC field appears weaker. This might be the result of poorer resolution of the NMC data, and the AMEX data is consistant with the fields analyzed by Gunn *et al.* (1989).

Figures 2.14 a–b show the NMC derived zonal winds and potential vorticity for the sector. Here, the difference in velocity appears again. Compare Fig. 2.14a to Fig. 2.9a. In the AMEX wind field (Fig. 2.9a), the values of easterly wind velocities are 20 ms^{-1}, while in the NMC field, the values are only 8 ms^{-1}. The differences are also visible in the westerlies.

These differences manifest themselves in the calculated potential vorticity field, Fig. 2.14b. Here, the relative values are only 1/2 of the AMEX values, and the maximum values are found higher in the atmosphere. With weaker wind flow, the potential vorticity would be calculated weaker, and it appears that the NMC anomalies are higher up because the vertical gradient of zonal wind is stronger than the horizontal gradient. This is not the case in the AMEX data.

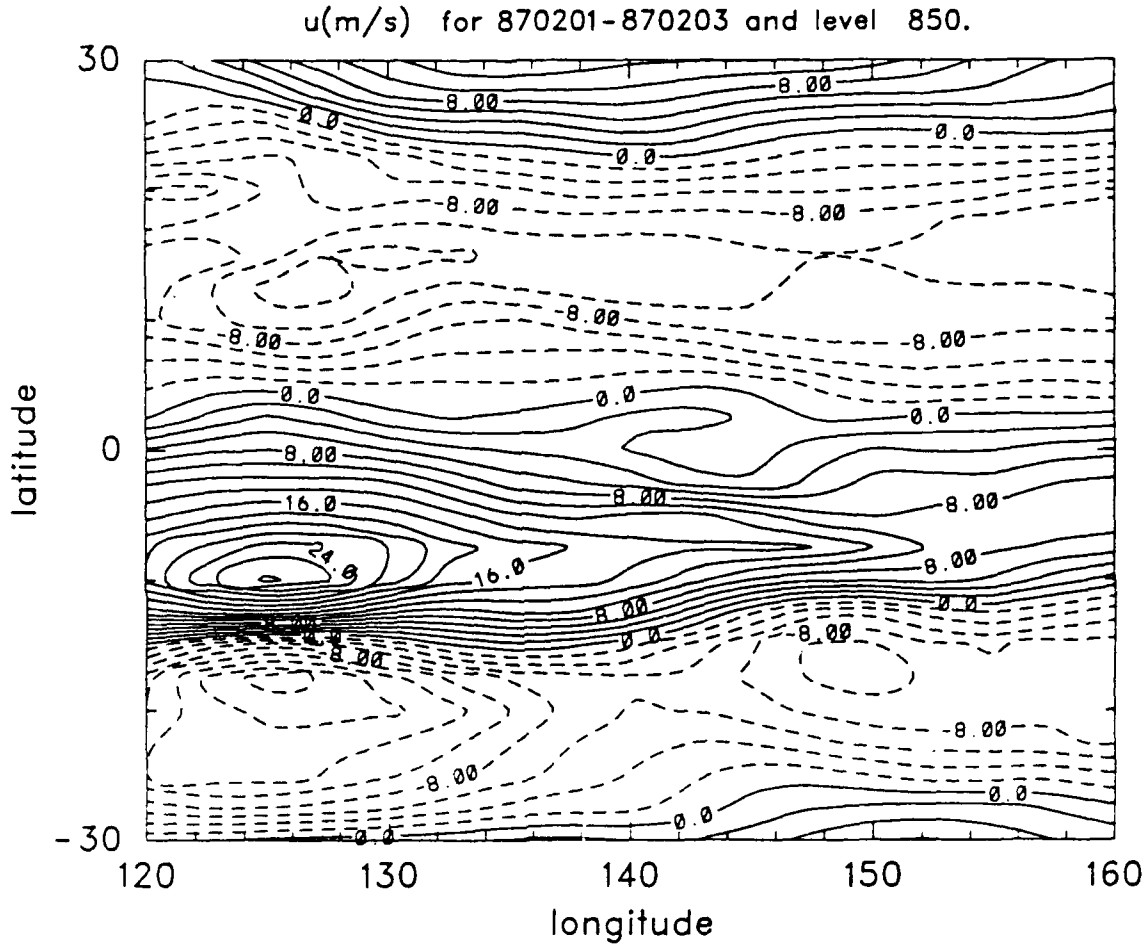

Figure 2.13: Zonal winds for 2/1/87 - 2/3/87 at 850 mb from NMC data. Units are ms^{-1}.

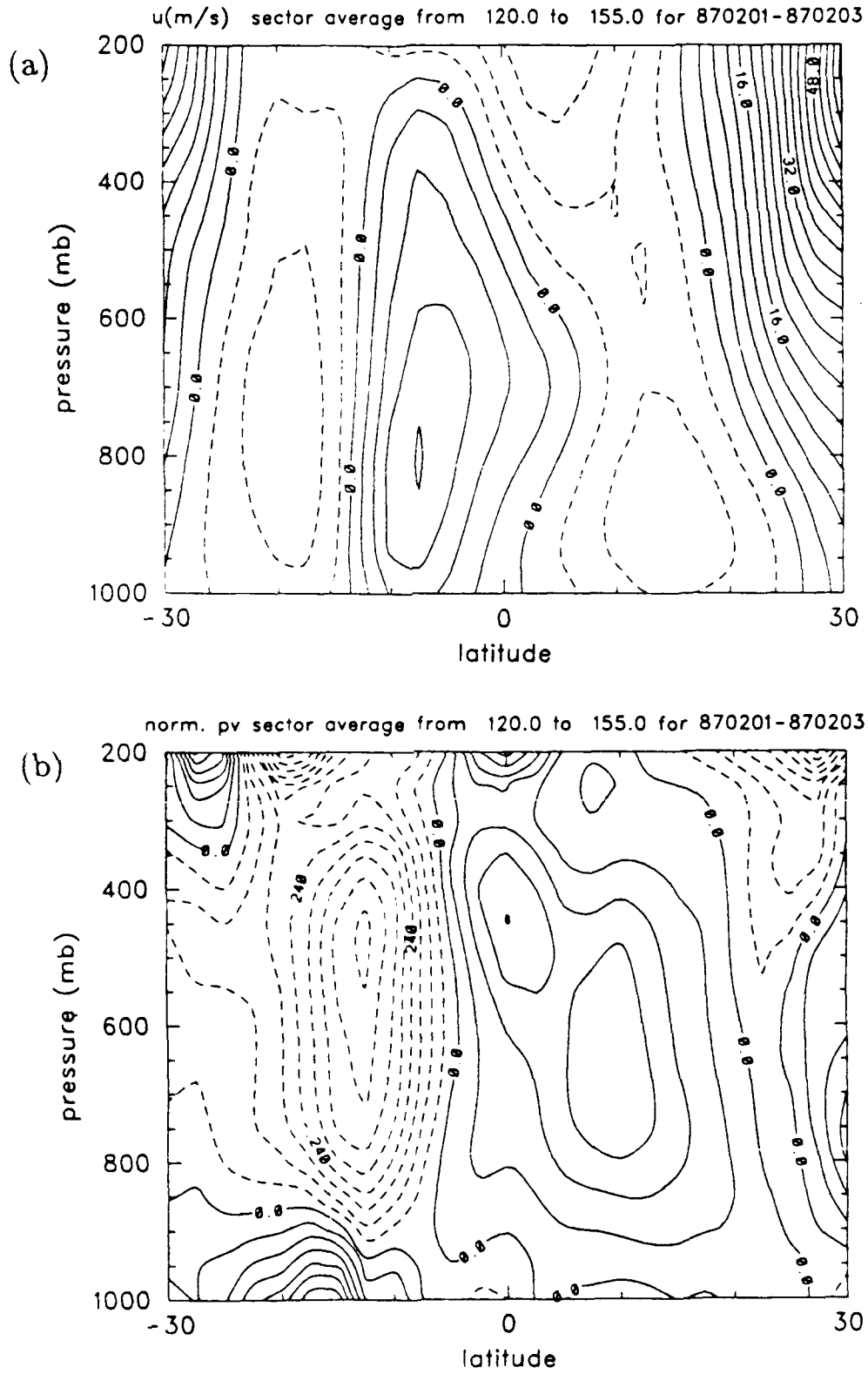

Figure 2.14: Sector averaged cross section for 2/1/87 - 2/3/87 of (a) zonal winds (ms^{-1}) and (b) normalized potential vorticity. NMC data.

Looking now at Figs. 2.15 a-b, the 15 day sector averages, again the NMC difference is apparent. The NMC zonal winds are nearly 1/2 the magnitude of the AMEX zonal winds in Fig. 2.11b. This causes the potential vorticity displayed in Fig. 2.15b to be weaker than the AMEX case (Fig. 2.12). Still, the structure is similar, and both data sets show that the area of reversed gradient is present.

One interesting feature present in the NMC potential vorticity calculations is the presence of an area of relative maximum potential vorticity in the northern hemisphere, located at 5 degrees north. This area should correspond to the descending portion of the Hadley cell, and one would not expect there to be enough convection to cause an increase of potential vorticity. While convection is not the only way to increase potential vorticity in this northern area, it is a possible cause. In this area, the sea surface temperatures are very warm, even in the winter. Convection is a year-round event in this area. Since the convection is continually occurring, there may be enough build up of potential vorticity over time to cause such an anomaly. Indeed, there are tropical cyclones every month of the year in the west Pacific, so the idea of this convection should not be hard to accept.

Another interesting area to investigate would be the eastern Pacific ocean, for the time frame documented by Hack *et al.* (1989). This area has a strong ITCZ, and Hack *et al.* analyzed a case of ITCZ breakdown they attributed to potential vorticity anomalies. There are two problems with this area. First, the data is very sparse, and second, it is obvious that the NMC data is not good enough to resolve the important circulations as seen previously in this paper. With these two problems considered this area would be very difficult to analyze correctly.

2.4 Modelling Results

The work in the previous section has suggested that the potential vorticity anomaly in the winter (northern) hemisphere could be a result of secondary convective forcing that occurs over the relatively warm west Pacific waters. One way to test this assumption is to model the ITCZ circulations, and put a secondary, smaller convective parameterization in the northern hemisphere. The model used has been previously described by Schubert

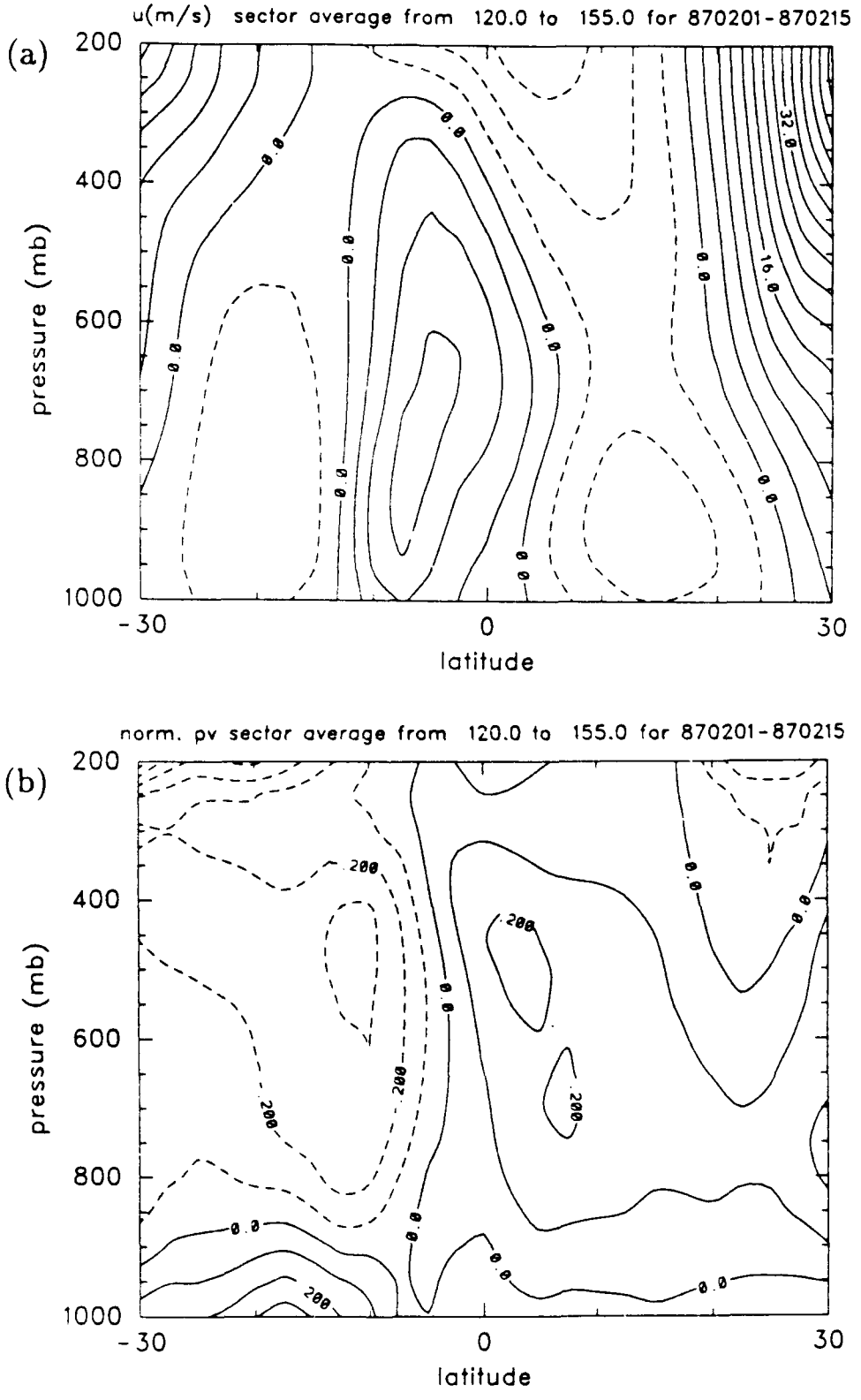

Figure 2.15: Sector averaged cross section for 2/1/87 - 2/15/87 of (a) zonal winds (ms^{-1}) and (b) normalized potential vorticity. NMC data.

$$P\sigma^* = 2\Omega \sin \Phi \ , \tag{2.8}$$

where P is the potential vorticity and Φ is the potential latitude defined by $\sin \Phi = \pm \left(1 - U \cos \phi / \Omega a \sin^2 \phi\right)^{1/2} \sin \phi$. Potential latitude is interpreted as the latitude you would have to move an air parcel, conserving angular momentum, so that the parcel's zonal wind component vanishes. The two root equation indicates that two latitudes (one north, the other south) will satisfy the equality.

The first case run was with an ITCZ centered at 10 degrees south, and no convection in the northern hemisphere. Figure 2.16a is a representation of the normalized potential vorticity after 6 model days of convective forcing. The areas of reversed potential vorticity gradients are stippled. The mid-tropospheric area of reversed gradient corresponds well to the previous section's plots. One feature represented in the model, but not in the NMC-based calculated fields is the area of reversed gradient above and equatorward of the main, middle level anomaly. Schubert *et al.* (1991) hypothesized this area was advected to this position by the Hadley circulation. This area, corresponding to a pressure height of 100 mb, is above the top of the NMC calculated plots from the previous section, but appearing in the AMEX plots. This area of interest at 100 mb also appears quite small when compared to the main area of reversal. It is possible that the NMC data is not fine enough to resolve this feature, or that it is just too far above the highest level calculated. Figure 2.16b shows the associated wind field obtained by inverting the potential vorticity field. The narrow, moderately strong band of westerlies are evident in the model run just between the ITCZ at 10 south and the equator. This is just where the westerlies appeared on the data plots in the previous section.

The next case explores the situation with convection in the northern hemisphere. The potential vorticity field presented in Fig. 2.17a is the result of an ITCZ at 15 degrees south, and a secondary forcing located at 5 degrees north, with 1/2 the magnitude of the main ITCZ forcing. Indeed, a second, smaller area of reversal potential vorticity gradient does appear in response to this convection. Note also that this is after 9 model days. The time

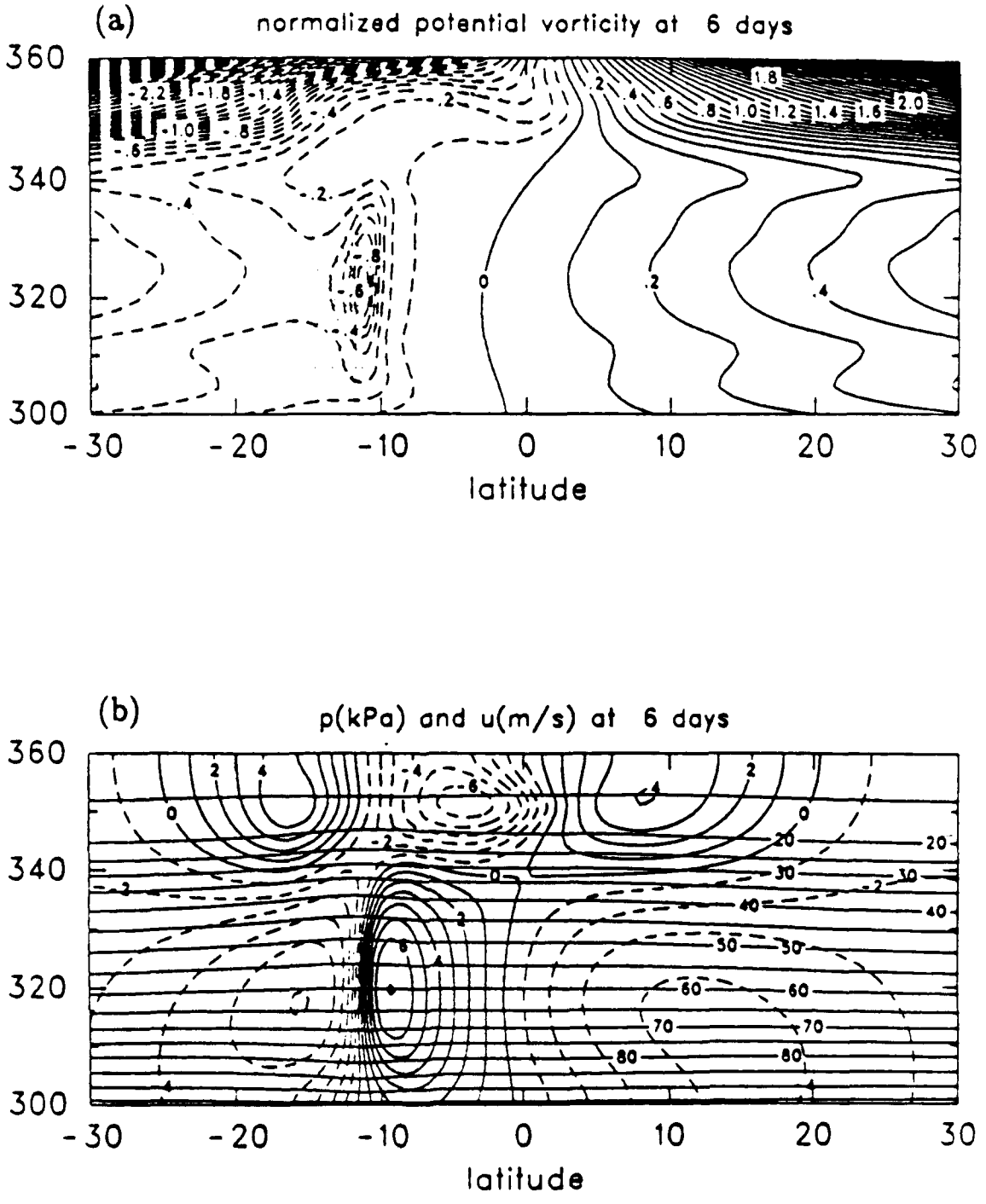

Figure 2.16: Hadley cell model derived (a) normalized potential vorticity at 6 model days and (b) zonal wind field at 6 model days (ms^{-1}). ITCZ located at 10 south.

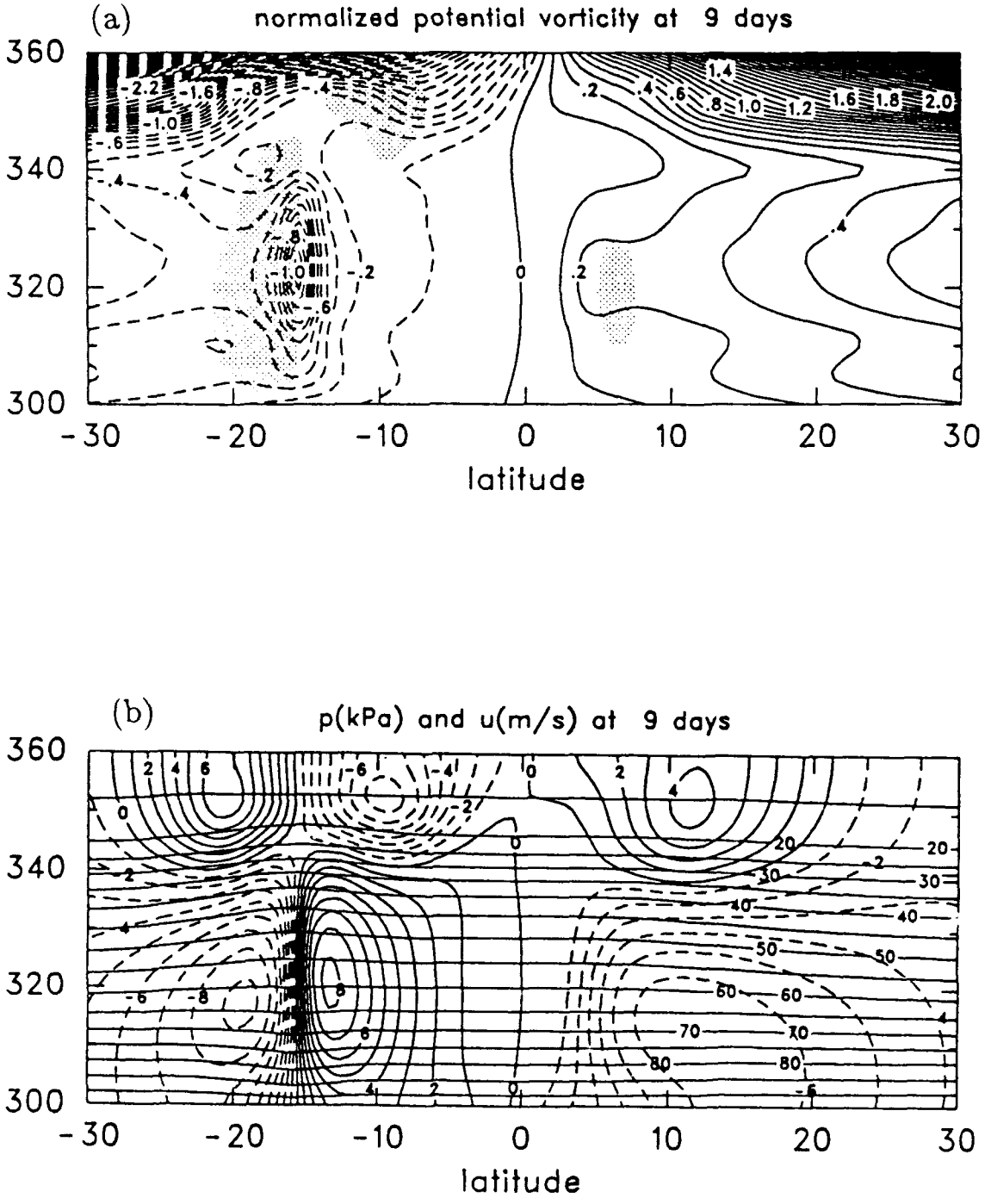

Figure 2.17: Hadley cell model derived (a) normalized potential vorticity at 9 model days and (b) zonal wind field at 9 model days (ms^{-1}). ITCZ at 15 degrees south with secondary forcing at 5 degrees north.

to generate this second area is not unreasonable. Since there is nearly always convection in this northern hemisphere area, the anomaly builds slowly, and then maintains itself, never reaching a critical enough value to cause a breakdown of organized convection as occurs in the summer hemisphere. There is also no corresponding upper anomaly in the northern hemisphere, again supporting the theory that the upper level area of reversal is indeed advected there by the Hadley circulation. Figure 2.17b shows the wind and pressure field obtained by inverting the potential vorticity in Fig. 2.17a. Again, westerlies are evident between the ITCZ and the equator, but absent are any corresponding northern hemisphere westerlies. This suggests that the convection in the northern hemisphere is indeed weaker. Also by comparing Fig. 2.17b and Fig. 2.15a, the sector averaged zonal wind, it is evident that the data show very weak northern hemispheric westerlies north of 28 degrees. It is our belief that the model approximates the situation well, and indeed, the secondary convection in the northern hemisphere is a possible explanation of the observed northern hemisphere potential vorticity anomaly. The main point to stress, however, is that this area of reversed gradient in the northern hemisphere is much weaker that the ITCZ-produced anomaly.

Chapter 3

BALANCE APPROXIMATIONS IN THE TROPICAL ATMOSPHERE

The overall goal in atmospheric science is to increase our knowledge of how the atmosphere operates. Despite the breadth of scale, from cloud drops to planetary waves, this increased understanding is often used to make better predictions of some future state of the atmosphere. Problems arise, however, due to the complicated nature in which the atmosphere moves and the way it reacts to solar and oceanic inputs of energy.

For numerical weather prediction, the primitive equations work over the entire globe however their complexity renders the results difficult to interpret. For physical insight into a particular phenomenon, reduced sets of equations are used where unimportant motions are filtered from the system. For large scale, midlatitude phenomena, the quasi-geostrophic system works well. On the other hand, in the tropics where the Coriolis force, $f = 2\Omega \sin \phi$, is small and changes sign, this system is no longer valid. The discussion which follows in this chapter describes some of the more prominent dynamical theories that have been proposed for studying large-scale tropical motions. Although not all inclusive, this discussion should provide sufficient motivation for considering the present scheme which will be evaluated in detail in the next chapter.

3.1 Matsuno (1966)

In 1966, Matsuno investigated tropical motions with the intention of analyzing these motions with quasi-geostrophic filtering. This approach at middle latitude separates the motion into two types: inertia-gravity waves and Rossby waves. Since the Rossby waves carry most of the energy of the large scale flow, the gravity waves are filtered out. Matsuno showed that the distinctions between gravity waves and Rossby waves are not always obvious in the tropical regions. The main difference in the middle latitudes is that the

gravity waves have a much higher frequency than the Rossby waves do. Matsuno found that this is not always the case in tropical regions.

After solving his equations, dispersion diagrams were produced as in Fig. 3.1. For non-zero positive index n, which corresponds to meridional wave number, there is a clear separation between the two inertia-gravity waves (one westward moving, the other eastward moving) and the Rossby waves. The problem Matsuno encountered was the existence of a peculiar eastward propagating wave with $n = 0$. For small zonal wavenumbers, this wave has the characteristics of a Rossby wave, but at large zonal wavenumbers it has the appearance of a gravity wave. Therefore, by using time scaling arguments, the allowed solutions would exclude this mixed Rossby-gravity wave. Matsuno concluded that quasi-geostrophic methods of filtering would not be appropriate near the equator.

An interesting sidelight of Matsuno's work can be seen in Fig. 3.1. The dark dashed line corresponds to n = -1. Matsuno's solutions correctly predicted a Kelvin wave-type structure. He noted this wave acts as a pure gravity wave which propagates in the eastward direction, and thus would be filtered out in his system. Not until Wallace and Kousky's (1968) work did evidence exist for Kelvin waves in the atmosphere. Kelvin waves were known to exist in the oceans near the coastlines, dying out away from the coast, but direct observational evidence for them in the atmosphere was not found until 1968. Wallace and Kousky (1968) noted that the Kelvin waves produced an upward flux of westerly momentum into the stratosphere, and linked this to the westerly phase of the Quasi-Bienniel Oscillation (QBO). This Kelvin wave acts as a pure gravity wave in the zonal direction. Due to its significance in tropical dynamics it would be improper to filter out this wave in the study of large-scale tropical phenomena. Matsuno correctly concluded that the quasi-geostrophic system would not work for understanding tropical motions.

3.2 Moura (1976)

Moura (1976) used the so called 'bal · equations' in his study of tropical motions. The simplifications made to the primitive equations include replacing the divergence equation with a diagnostic relationship between the horizontal nondivergent velocity and the

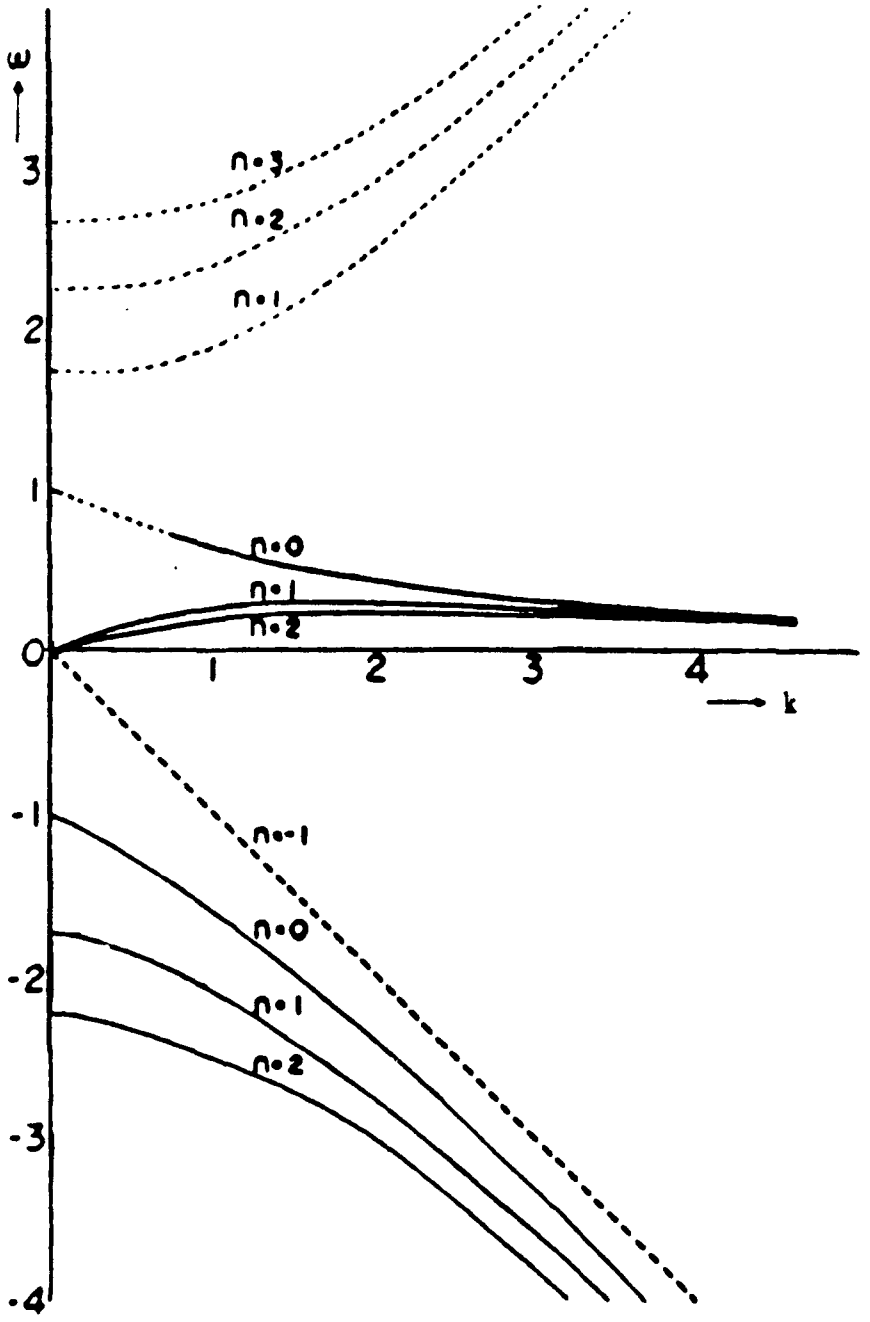

Figure 3.1: Frequencies as functions of wavenumber. Thin solid line: eastward propagating inertio-gravity waves. Thin dashed line: westward propagating inertio-gravity waves. Thick solid line: Rossby (quasi-geostrophic) waves. Thick dashed line: The Kelvin wave like wave. (Matsuno, 1966).

horizontal variations in the mass field. The assumption is that the horizontal divergence is negligible for large scale motions. This is quite valid in the tropics, where the vertical motion field is small outside regions of precipitation.

The advantage of Moura's filtered system was that it did not treat gravity waves, and for numerical integration, longer time steps could be used. Again, the problem of the missing Kelvin waves is encountered when gravity waves are filtered. Moura realized this, and tested the so called 'modified balance equations' derived by Charney in 1962. These modified equations include a term proportional to beta and the x-derivative of velocity potential. These new equations allow Kelvin waves, in addition to many spurious gravity waves. These solutions were in the form of high frequency waves, and thus a small time step was required in the computation. Moura suggested that there might be an iterative scheme to remove the unwanted gravity waves, while at the same time, keeping the Kelvin waves. Moura was unable to find such a technique. The problem of finding good approximations to the primitive equations in a balance system was clearly not resolved by Moura (1976). He stated "...if one does not devise an efficient method to get rid of these high frequency modes, it would seem hardly acceptable to use these equations in numerical models for practical purposes."

3.3 Gill (1980)

Gill (1980) performed a simple numerical experiment to study the Kelvin wave's role in the equatorial eastern Pacific easterly wind field. In the process, he formulated a model that reproduced many of the prominent flow features in the tropics.

Like Matsuno (1966), Gill used the divergent shallow water equations on an equatorial beta-plane to represent the horizontal structure. To keep the model simple, only one vertical mode was allowed. The changes made to the Matsuno model by Gill involved the inclusion of both forcing and dissipation terms, and making the long wave approximation. This long wave approximation involves the neglect of the meridional acceleration term in the zonal momentum equation to allow a balance between the Coriolis force and the meridional pressure gradient force. By neglecting meridional accelerations, gravity waves

are excluded; the Kelvin wave, with only zonal motion, is retained. Gill placed the forcing functions in his model to represent convection in the Indonesian area. With this forcing, the model produced easterly flows at low levels east of the convection area, consistent with observations in the equatorial Pacific Ocean. The easterly flow was just part of a larger circulation that looked very much like the Walker circulation. Also present were low level westerly flows in an area that corresponded to the Indian Ocean, again consistent with observations. Both of these wind regimes can be explained by the propagation of waves away from the convective forcing area: the westerlies by propagation of planetary Rossby waves, and the easterlies by the propagation of Kelvin waves.

While Gill's model formulation is a simplistic view of the tropical atmosphere, it did confirm the importance of Kelvin waves and show that general features of the tropics could be produced by a relatively simple model.

3.4 Stevens *et al.* (1990)

We now consider the balance system proposed by Stevens *et al.* (1990) which is a generalization of Gill's model to include vertical stratification and spherical effects. The equations of zonal and meridional momentum, hydrostatic approximation, continuity equation, and thermodynamic energy equation are as follows

$$\frac{DM}{Dt} = -\frac{\partial \Phi}{\partial \lambda} + F \,, \tag{3.1}$$

$$\delta \frac{Dv}{Dt} + \frac{u^2 \tan\phi}{a} + (2\Omega \sin\phi)\, u = -\frac{\partial \Phi}{a \partial \phi} \,, \tag{3.2}$$

$$\frac{\partial \Phi}{\partial z} = G(z)\theta \,, \tag{3.3}$$

$$\frac{\partial(\rho u)}{a \cos\phi \partial \lambda} + \frac{\partial(\rho v \cos\phi)}{a \cos\phi \partial \phi} + \frac{\partial(\rho \omega)}{\partial z} = 0 \,, \tag{3.4}$$

$$\frac{D\theta}{Dt} = Q \,, \tag{3.5}$$

$$\frac{D}{Dt} = \frac{\partial}{\partial t} + \frac{u}{a\cos\phi}\frac{\partial}{\partial\lambda} + \frac{v}{a}\frac{\partial}{\partial\phi} + \omega\frac{\partial}{\partial z} \ , \tag{3.6}$$

where $(u,\ v,\ w)$ are the velocity components in the (eastward, northward, upward) directions and $M = a\cos\phi(\Omega a\cos\phi + u) \equiv$ angular momentum per unit mass, Φ = geopotential, F = zonal body torque, a = radius of the earth, λ = latitude and ϕ = longitude. Following the lead of Stevens *et al.* the vertical coordinate, z, can represent several different vertical coordinate system. While the actual choice of the vertical coordinate is not important, the primary point here is that the density, $\rho(z)$, and the hydrostatic proportionality coefficient, $G(z)$, are functions only of this coordinate.

The actual balance approximation is given by Eq. (3.2), when the balance tracer (δ) is set equal to zero. This leads to a balance between the zonal wind and the meridional pressure gradient force. The usually small curvature term is left in to formulate conservation laws for energy and potential vorticity.

The absolute vorticity vector was defined as

$$\zeta = (\xi,\ \eta,\ \zeta) = \left(-\delta\frac{\partial v}{\partial z}, \frac{\partial u}{\partial z}, 2\Omega\sin\phi + \frac{\delta\partial v}{a\cos\phi\partial\lambda} - \frac{\partial(u\cos\phi)}{a\cos\phi\partial\phi}\right) \ , \tag{3.7}$$

and the three-dimensional divergence by

$$\nabla\cdot u = \frac{\partial u}{a\cos\phi\partial\lambda} + \frac{\partial(v\cos\phi)}{a\cos\phi\partial\phi} + \frac{\partial\omega}{\partial z} \ , \tag{3.8}$$

which leads to

$$\frac{D\xi}{Dt} = (\zeta\cdot\nabla)u - (\nabla\cdot\boldsymbol{u})\xi + \frac{G}{a}\frac{\partial\theta}{\partial\phi} + \frac{\tan\phi}{a}\frac{\partial}{\partial z}\left(\frac{u^2}{2} + \delta\frac{v^2}{2}\right) \ , \tag{3.9a}$$

$$\frac{D\eta}{Dt} = (\zeta\cdot\nabla)u - (\nabla\cdot\boldsymbol{u})\eta - \frac{G}{a\cos\phi}\frac{\partial\theta}{\partial\lambda} + \frac{1}{a\cos\phi}\frac{\partial F}{\partial z} \ , \tag{3.9b}$$

$$\frac{D\zeta}{Dt} = (\zeta\cdot\nabla)u - (\nabla\cdot\boldsymbol{u})\zeta - \frac{1}{a\cos\phi}\frac{\partial F}{a\partial\phi} \ . \tag{3.9c}$$

Note that there is no vertical velocity in the vorticity vector. By making the balance approximation, δ equals zero in Eq. 3.9a, the zonal component of the vorticity vector

disappears. Thus the vorticity vector lies in the meridional plane and is dependent only on the zonal portion of the flow.

The next task is to derive a potential vorticity relationship. By using the above vorticity vector and the continuity (3.4) and thermodynamic (3.5) equations, the following is obtained:

$$\zeta \cdot \nabla\theta = -\delta \frac{\partial v}{\partial z}\frac{\partial \theta}{a\cos\phi\partial\lambda} + \frac{\partial u}{\partial z}\frac{\partial\theta}{a\partial\phi} + \left(2\Omega\sin\phi + \frac{\delta\partial v}{a\cos\phi\partial\lambda} - \frac{\partial(u\cos\phi)}{a\cos\phi\partial\phi}\right)\frac{\partial\theta}{\partial z} . \quad (3.10)$$

Stevens notes that some manipulation leads to

$$\rho\frac{Dq}{Dt} = \zeta\cdot\nabla Q + \frac{i\cdot(\nabla\theta\times\nabla F)}{a\cos\phi} . \quad (3.11)$$

Equation (3.11) is a relationship for the conservation of potential vorticity.

In 1985, Hoskins *et al.* stressed the importance of "potential vorticity thinking" as a key in understanding large scale dynamical processes. With a given potential vorticity field, it is possible, with the appropriate boundary conditions, to 'invert' the potential vorticity field to get the primary flow features (such as wind and temperatures). While this is most helpful in the middle latitudes, a possible problem arises in the tropics. The equatorially trapped Kelvin wave can explain the easterly flow found in the eastern tropical Pacific, and plays an important role in the QBO. The difficulty is that the Kelvin wave has zero potential vorticity. Thus by calculating the potential vorticity field and inverting it, the flow features associated with the Kelvin wave would be missed. Therefore, Schubert *et al.* (1991) suggest that it may better to predict some other variable, one that contains all of the flow features. Such a variable might be angular momentum or potential temperature. This limitation due to the 'invisible' Kelvin waves should not detract from the attractiveness of the proposed quasi-balanced scheme. Indeed, potential vorticity thinking in the tropics may prove useful in understanding wave growth (as in the previous chapter) or, inverse potential vorticity in the form of potential pseudodensity, may prove useful in defining the tropopause at all latitudes, thus uniting the tropics and middle latitudes together in one prediction scheme (Stevens *et al.* 1990).

Chapter 4

DATA STUDY OF CURRENT THEORY

The validity of the quasi-balanced approximation as derived by Stevens *et al.* (1990) will be tested in this chapter. For an approximation to be valid it must first be mathematically correct by containing the basic conservation laws of atmospheric motion. Second the approximation must be physically reasonable, i.e., in the quasi-balanced approximation is the neglect of the meridional acceleration term physically justified?

The initial justification for the proposed balanced dynamical system comes from observations. Wallace (1983) showed that, in the area from the deep tropics to 45 degrees north, the zonal component of stationary wave kinetic energy dominates over the meridional kinetic energy component. This result suggests that for large, slowly evolving flow, there is physical justification to neglect the meridional acceleration processes when compared to the zonal scale. This does not mean that meridional accelerations are unimportant. In Kelvin waves, meridional acceleration terms are necessary to describe their structure. The result does suggest, however, that these meridional accelerations may be neglected when compared to processes that operate mainly in the zonal direction.

If this approximation is to be used to describe tropical motions and ultimately predict them, more specific questions should be asked such as: Are there certain areas and/or time scales that the approximation is more valid for? Does this approximation hold for large departures from normal tropical flow?

The first test of the quasi-balanced approximation involves isentropic potential vorticity. The equation for potential vorticity was presented as Eq. (3.10) and is repeated here:

$$\zeta \cdot \nabla\theta = -\delta \frac{\partial v}{\partial z} \frac{\partial \theta}{a \cos\phi \partial\lambda} + \frac{\partial u}{\partial z} \frac{\partial \theta}{a \partial \phi} + \left(2\Omega \sin\phi + \frac{\delta \partial v}{a \cos\phi \partial\lambda} - \frac{\partial (u \cos\phi)}{a \cos\phi \partial\phi} \right) \frac{\partial \theta}{\partial z} . \quad (4.1)$$

To test the validity of the quasi-balanced approximation, namely $\delta = 0$, potential vorticity calculations were made using the same AMEX data set and same times as those presented in chapter two. The calculations in chapter two used the full equation; the ones presented here use the quasi-balanced form of Eq. (3.10). With the emphasis placed on 'potential vorticity thinking', this comparison will show if this important variable can be properly calculated using the approximation form Eq. (4.1).

4.1 The Potential Vorticity Equation

From a first look at the quasi-balanced form of Eq. (4.1), it is obvious that the neglected terms will be small. With fairly uniform fields of potential temperature and small meridional velocities, the neglected term should be small. While this may not be an exciting scientific finding, the ability of the approximated equations to describe important flow features is important.

Figures 4.1 a–b show the approximated potential vorticity calculations for the active period of the Australian monsoon documented in chapter two of this thesis. Figure 4.1a should be compared to Fig. 2.8a. Not surprisingly the fields are nearly identical. Even with the different contour level, the areas of maximums and minimums are quite close. Comparison of Fig. 4.2 to Fig. 2.10 again shows good agreement. The calculation of potential vorticity using the quasi-balanced form of Eq. (4.1) clearly captures the important structure of this field. This result suggests that the approximated form of Eq. (4.1) is sufficient for the purpose of calculation of the isentropic potential vorticity field.

4.2 The Meridional Momentum Equation

In the realm of the quasi-balanced approximation, the meridional momentum equation is

$$\delta \frac{Dv}{Dt} + \frac{u^2 \tan\phi}{a} + (2\Omega \sin\phi)\, u + \frac{\partial \Phi}{a \partial \phi} = 0 \,. \tag{4.2}$$

By making the quasi-balanced approximation, we obtain

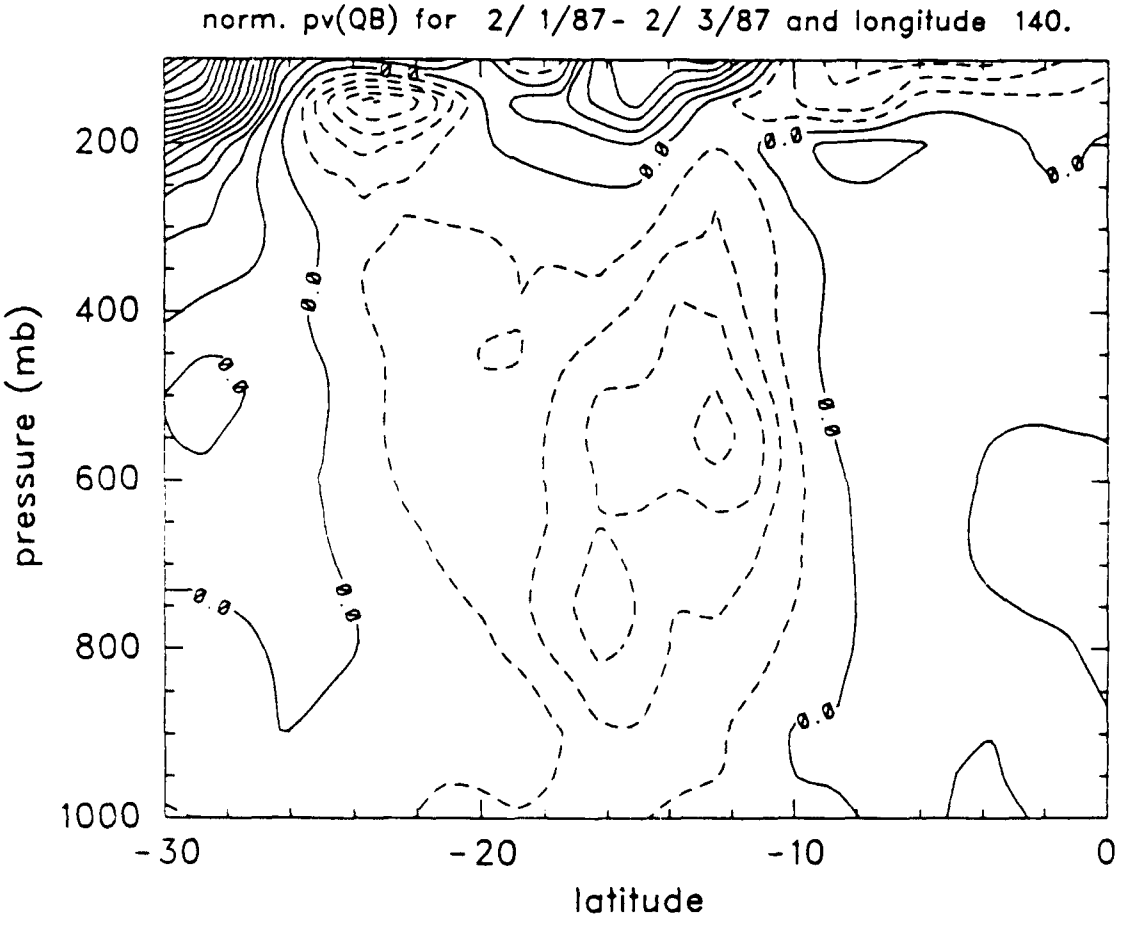

Figure 4.1: Normalized potential vorticity calculated using the approximation from ($\delta = 0$) of Eq. (4.1), for 2/1/87–2/3/87 and 140 degrees east longitude.

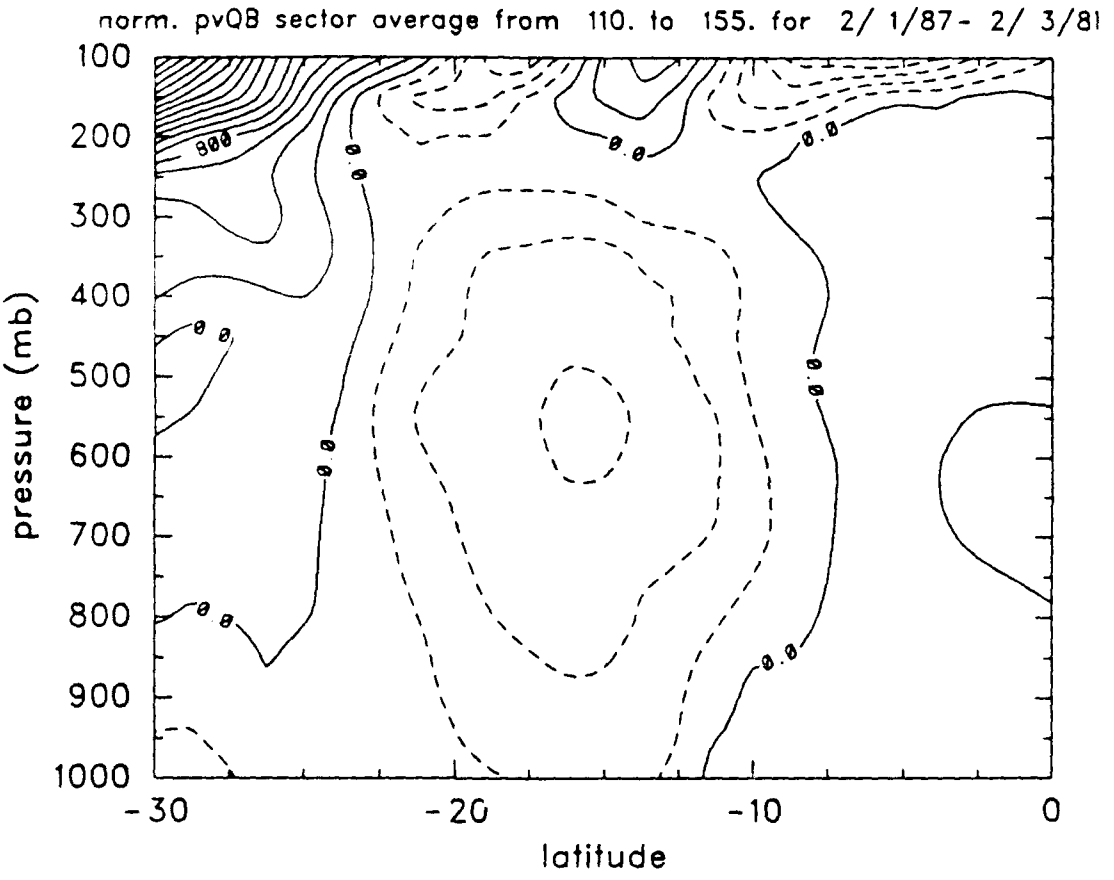

Figure 4.2: As in Fig. 4.1 except calculated for sector (110 to 155 degrees east longitude) average.

$$\frac{u^2 \tan\phi}{a} + (2\Omega \sin\phi)\, u + \frac{\partial \Phi}{a \partial \phi} = R \ , \tag{4.3}$$

where R is the residual. For exact balance, the residual would be identically zero. This residual term not only contains the neglected meridional acceleration term, but also other neglected terms such as surface and cumulus friction.

The first series of plots that will be presented here are representations of individual terms over the tropical atmosphere. National Meteorological Center archived global data was used with 2.5 degree resolution. The zonal wind speed and geopotential height were used to calculate individual terms in Eq. (4.3). These calculations were done at both 850 and 250 millibars, and also for different time averages of zonal wind and geopotential heights. The time chosen for the 'normal' state of the tropical atmosphere was January 1981 which was considered to be an average year in comparison to January 1982–83 when an ENSO event was present. At this time, the ENSO was nearing its maximum intensity.

Figures 4.3 and 4.4 are the individual terms from Eq. (4.3) at 250 and 850 mb, respectively. An uniform spatial structure in the residual field is present in both figures. Several features, however, do stand out. At 250 mb, the fields of curvature, Coriolis and pressure gradient force all show the winter hemisphere (northern) jet structure, while at 850 mb, the Coriolis and the pressure gradient force show the easterly trade winds in the central Pacific. While it is difficult to say many things qualitatively about the residual fields from these two figures, it is observed that most of the large gradients of positive residual occur over land. In the northern hemisphere, this suggests that the coriolis force *dominates*, or the pressure gradient force is not negative enough. Over land, in the winter hemisphere, high pressure tends to dominate, except for the times when intense middle latitude cyclones transit the continents. Both of these features, the strong high pressure and the deep low pressure systems should have associated with them appreciable gradients of meridional acceleration. In such cases, the neglect of this acceleration, which may appear quite far into the tropics due to the strength of the disturbances, is not appropriate. There may be some momentum mixing from the middle latitudes into the tropics due to these strong synoptic features, but overall, this is not too important.

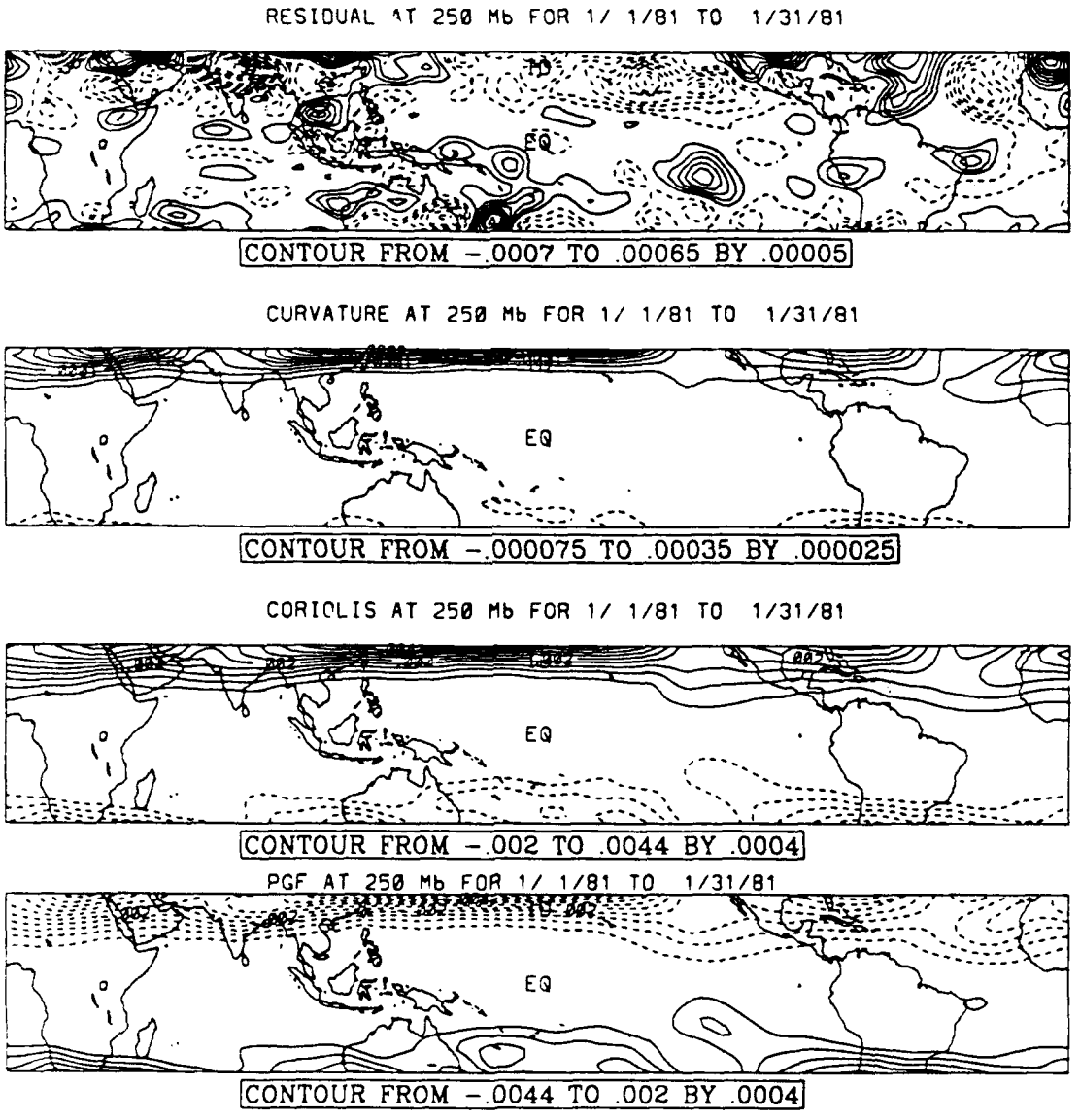

Figure 4.3: Thirty day average for January 1981, at 250 mb, plot of terms of equation (4.1). Units are ms^{-2}.

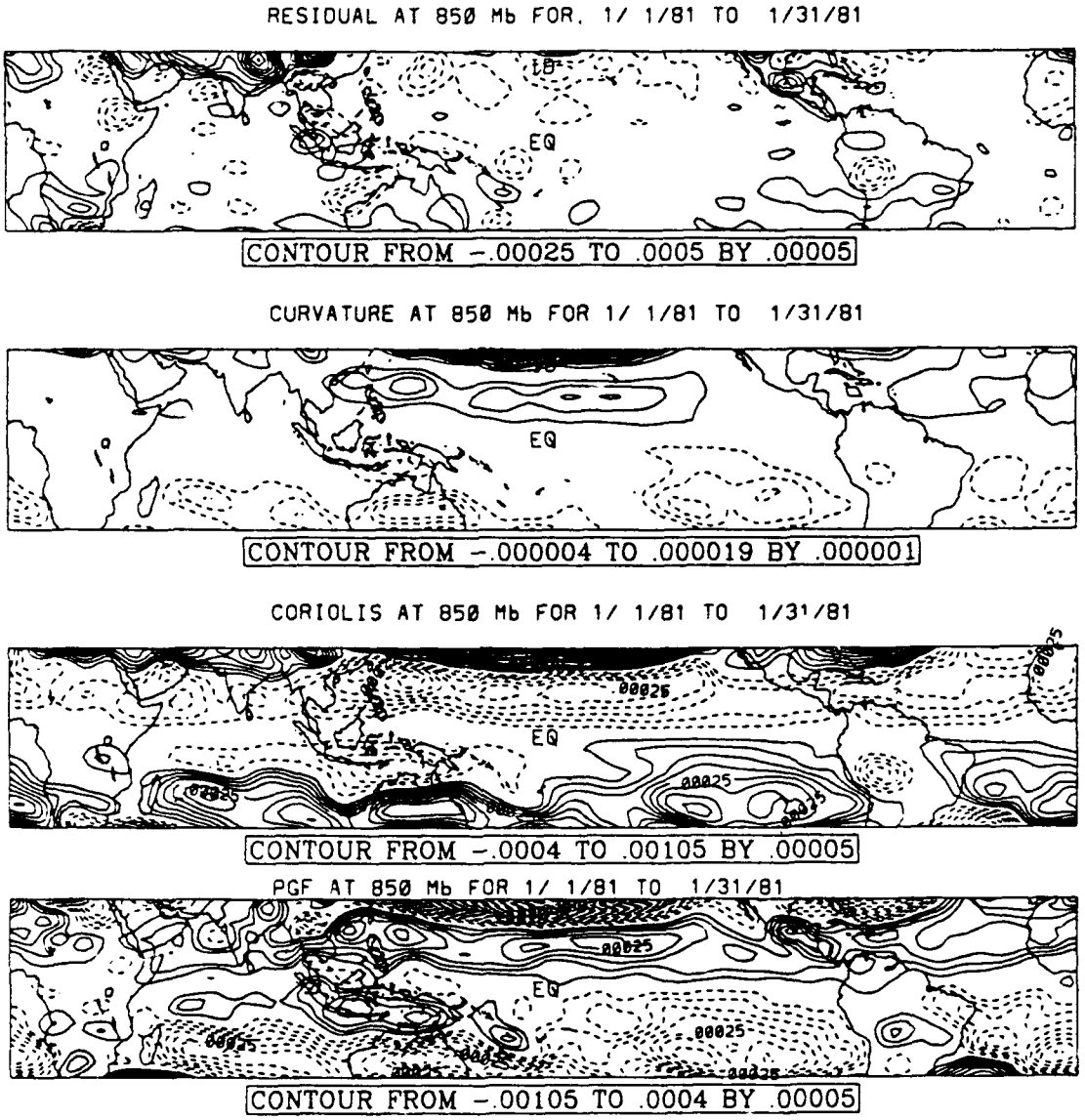

Figure 4.4: As in Fig. 4.3 except for 850 mb.

At 850 mb, the residual field appears somewhat less noisy than at 250 mb. The area over the Tibetan plateau should be regarded with some caution. North of 20 degrees latitude, the terrain rises sharply to heights well above 850 mb. What can be seen in Fig. 4.2 is that the residual field has a generally smaller magnitude that at 250 mb. If the main areas of residual over land are due to synoptic systems, and these systems reach their maximum intensity at the tropopause, then the residual at 250 mb should be larger. This is a possible explanation for the more complicated structure at 250 mb.

Figures 4.5 and 4.6 show the same terms, but at 10 day averages during January 1981. While not being too different from the 30 day averages, the 10 day averages do give a clue as to time scales of the residual field. The similarity between the 10 and 30 day fields suggests that the residual field reaches a kind of steady state by 10 days. A 5 day average (Fig. 4.7) residual field is more cluttered that the longer time averages, but still shows the same general shape as the longer averages. Many other time scales, from 12 hours (almost unreadable) to 60 days (quite smooth), were examined. While it is not possible to present all of these figures here, it appears that the residual field showed the most change between one and three days which suggests a possible time scale for this approximation. This is also consistent with the scaling arguments presented in Stevens *et al.* (1990), which pointed to a time scale of greater than 1/2 day. While the evolution of the residual field varied from case to case, depending on the pressure level and time of year, the steady state residual field was almost always reached by 3 days. Whether this is a result from the equivalent time scale of the approximation, or just the averaging process, cannot be determined at this time.

While showing the spatial pattern of the terms in the quasi-balanced approximation, Figs. 4.3-4.7 lack much detail about relative term sizes. By presenting north/south cross sections at a specific latitude, more information about the relative sizes can be seen. Figures 4.8 a-d show four cross sections. Two different longitudes are investigated. The first, 85 degrees longitude, was used to see the structure of the residual over the Tibetan plateau and the ITCZ which, during this period, is usually centered at about 10 degrees south. At most latitudes in Fig. 4.8a, the terms are quite comparable in size south of 10

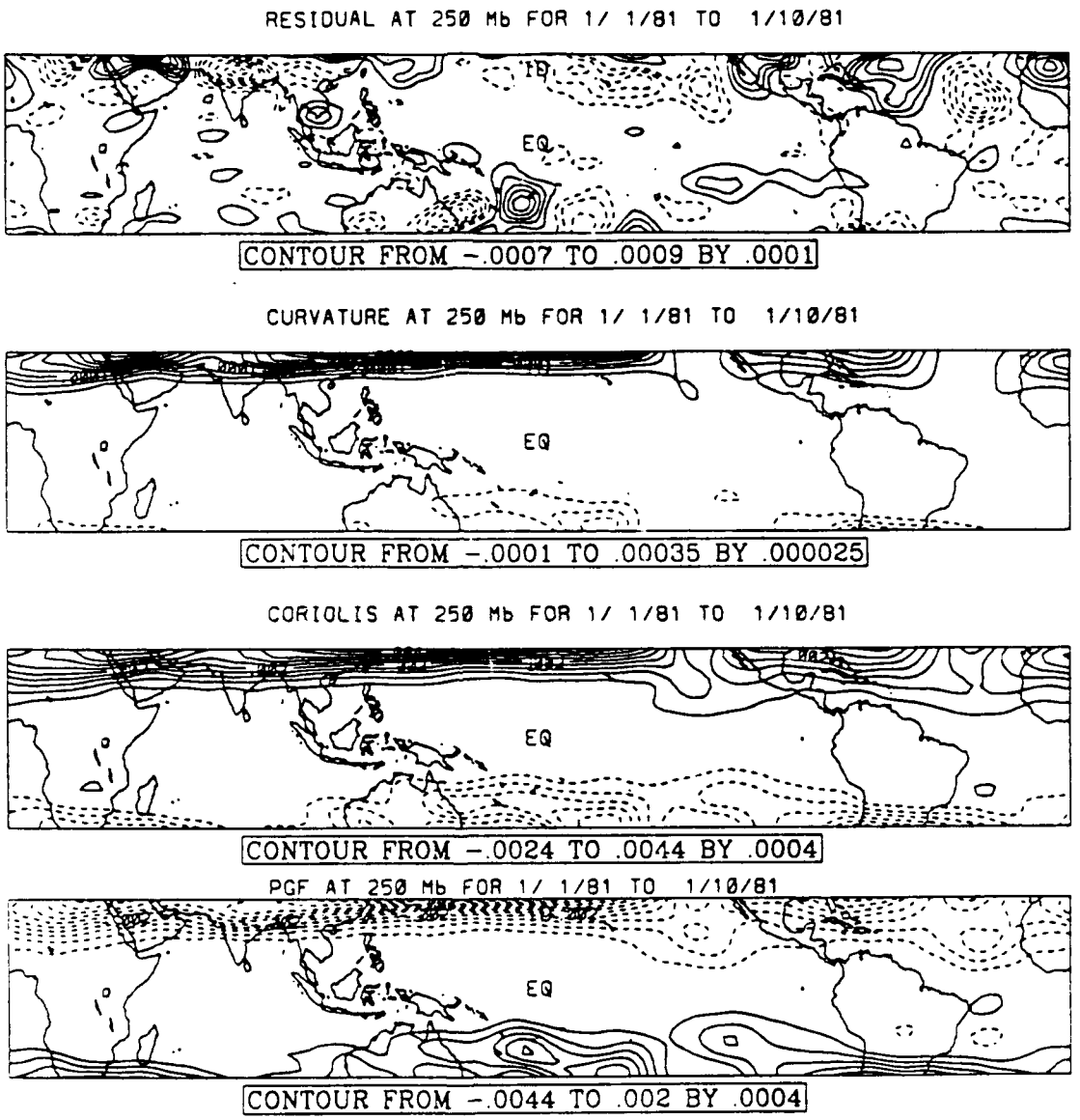

Figure 4.5: As in Fig. 4.4 except for 10 day average and 250 mb.

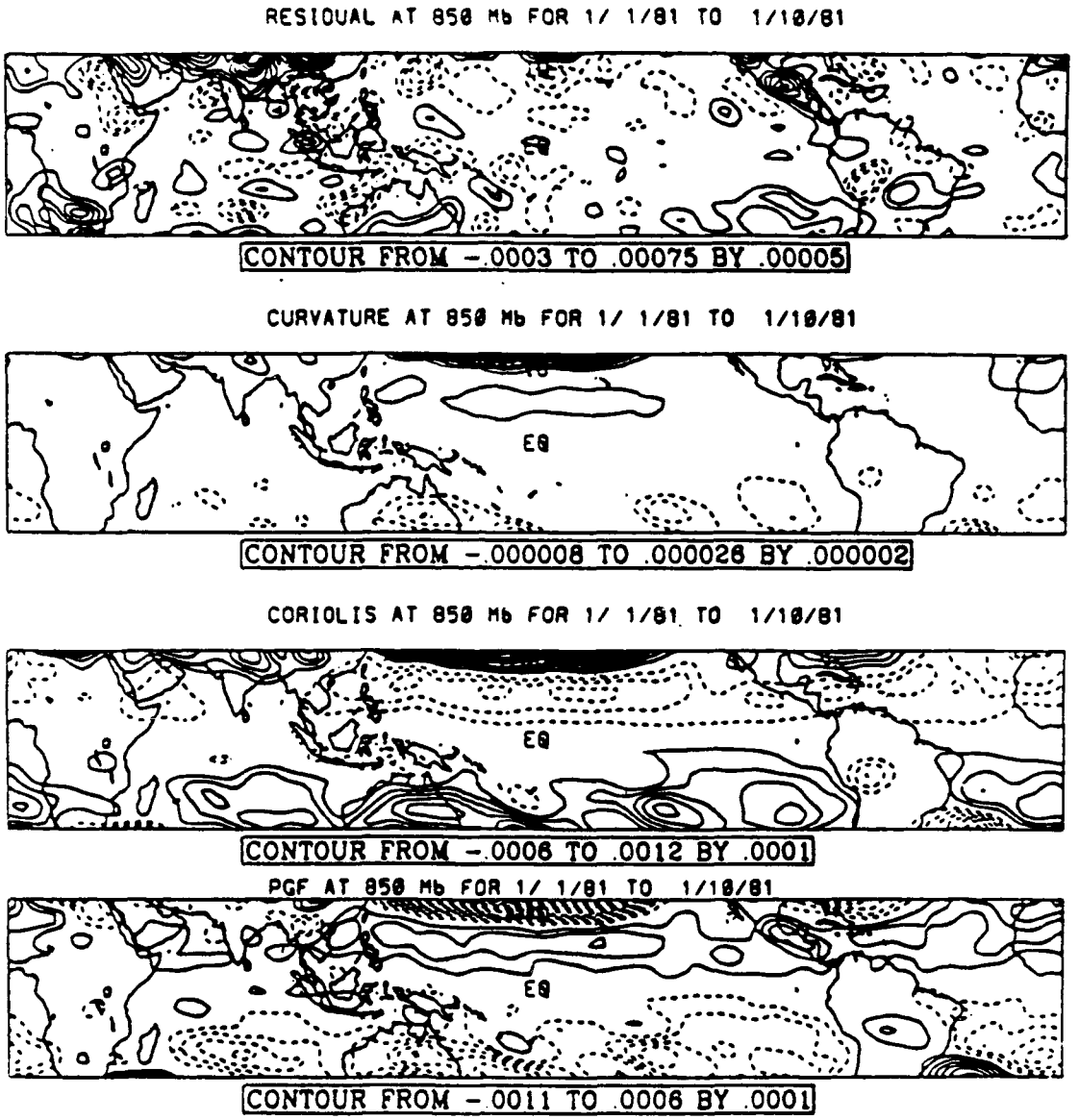

Figure 4.6: As in Fig. 4.5 except for 850 mb.

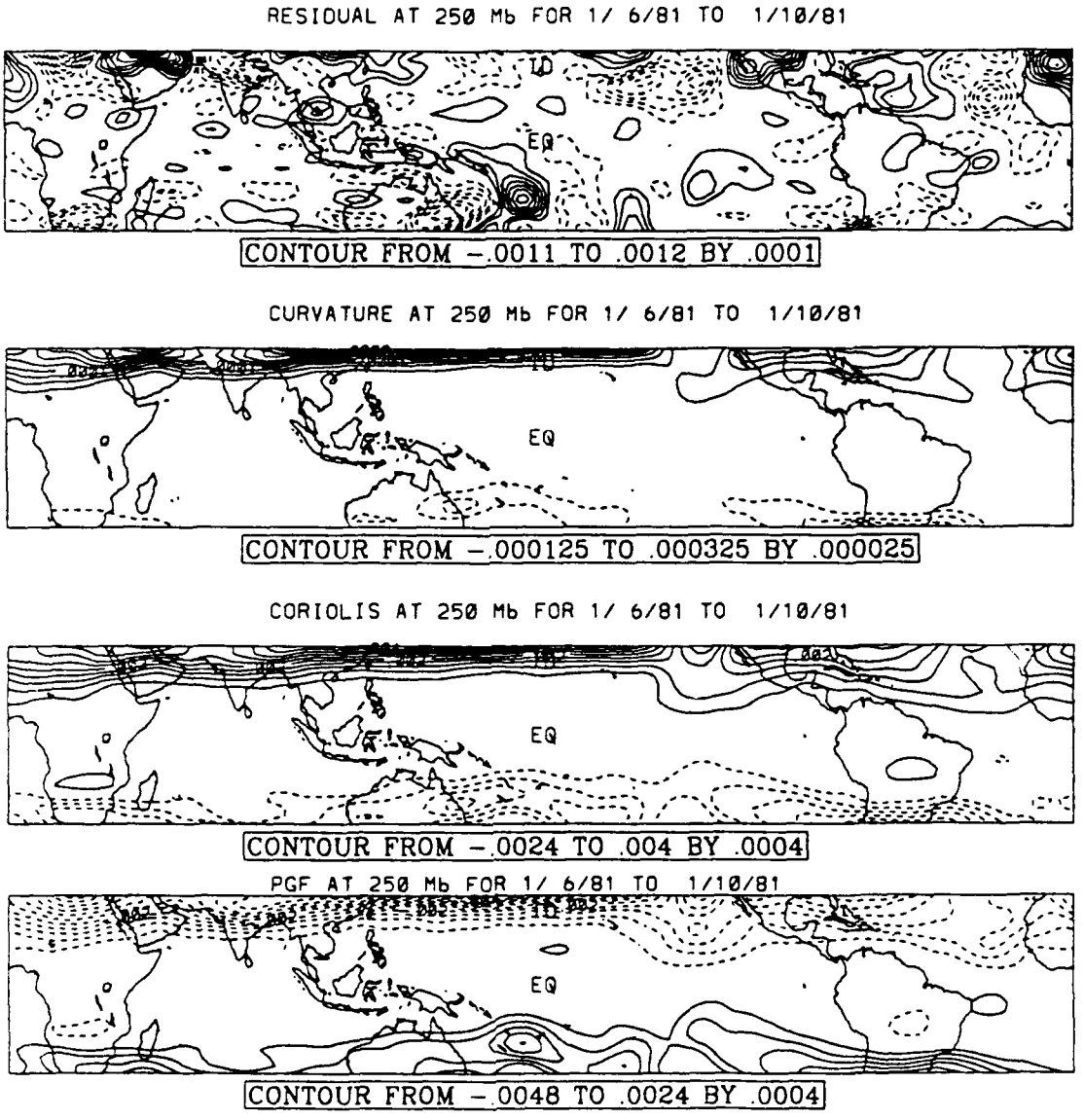

Figure 4.7: As in Fig. 4.5 except for 5 day average and 250 mb.

Figure 4.8: Thirty day average cross section of individual terms for January 1981 at (a) 85 degrees east and 250 mb, (b) 160 degrees east and 250 mb, (c) 85 degrees east and 850 mb and (d) 160 degrees east and 850 mb. *Units are* ms^{-2}.

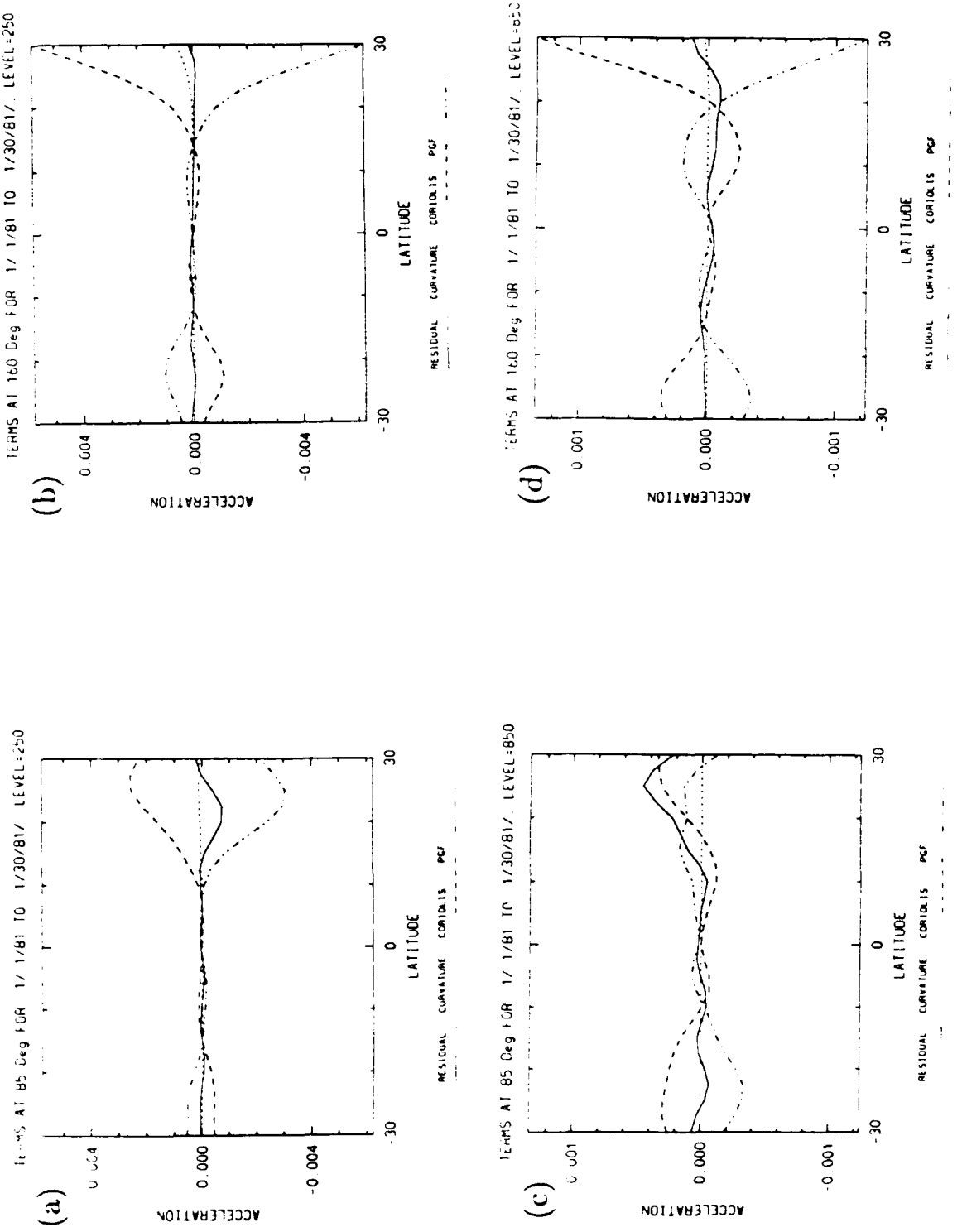
(a)
(b)
(c)
(d)
ACCELERATION
LATITUDE
RESIDUAL CURVATURE CORIOLIS PGF
0.004
0.000
-0.004
0.001
-0.001
30
0
-30

degrees north. Here the zonal wind is increasing, as seen by the increase in the pressure gradient force and Coriolis force. At approximately 15 degrees north, the pressure gradient force begins to dominate, and the residual becomes more negative. Figure 4.8b shows the terms at 160 degrees east. Here again, south of 10 degrees north, all of the terms are relatively small. Northward of this, both the pressure gradient and Coriolis forces are increasing, but unlike Fig. 4.8a, they approximately cancel each other out so as to keep the residual small. Figures 4.8 c-d shows the 850 mb level. Note again that north of 20 degrees north, terrain is higher than 850 mb and the plots north of this are meaningless. What should be noted about Figs. 4.8 c-d is that although the spatial structure of the residual fields was cleaner at 850 mb (Fig. 4.4), actually, the individual terms are more oscillatory than at 250 mb.

Figure 4.9 a-d shows the 10 day averages at the same locations. Figure 4.9 is similar to Fig. 4.8 in that it shows the residual term is generally smaller that the other two balance terms (pressure gradient and Coriolis forces). It is hard, however, to see exactly what is going on near the equator. In this region all of the terms are quite small, making it difficult to justify the quasi-balanced approximation. In order to compare the size of the residual term to the other terms near the equator, Fig. 4.10 shows a ratio between the residual and the largest term (pressure gradient or Coriolis force). The closer the ratio is to zero, the better the quasi-balanced approximation. Shown in these figures are ratios at 85 degrees longitude, as well as for the eastern Pacific basin from 120 degrees east to 160 degrees east. This basin ratio is presented after viewing separate longitude plots in this area and noting that they were similar. Any approximation of large scale motion, taken at a given point, may show small errors. Averaging over this larger domain should remove small perturbations from the large scale balance. Figure 4.10a shows the ratio at 85 degrees east and 250 mb. Note that against the commonly used '10% error criteria' the quasi-balanced approximation does poorly. Very few points are actually below the 0.1 level. It is of interest to note the spatial structure in this figure. Whereas in Figs. 4.8 and 4.9, the terms around the equator were small and hard to differentiate, in Fig. 4.10 the accuracy of the quasi-balanced approximation is easier to see. The most obvious feature

Figure 4.9: As in Fig. 4.8 except for 10 day average for January 1981 (a) 85 degrees east and 250 mb, (b) 160 degrees east and 250 mb, (c) 85 degrees east and 850 mb, and (d) 160 degrees east and 850 mb.

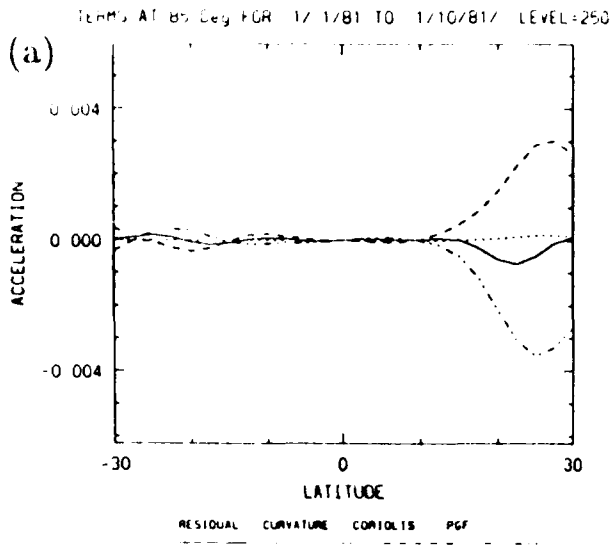
(a)
TERMS AT 85 Deg FOR 1/ 1/81 TO 1/10/81/ LEVEL=250
0 004
0 000
-0 004
ACCELERATION
-30
0
30
LATITUDE
RESIDUAL CURVATURE CORIOLIS PGF

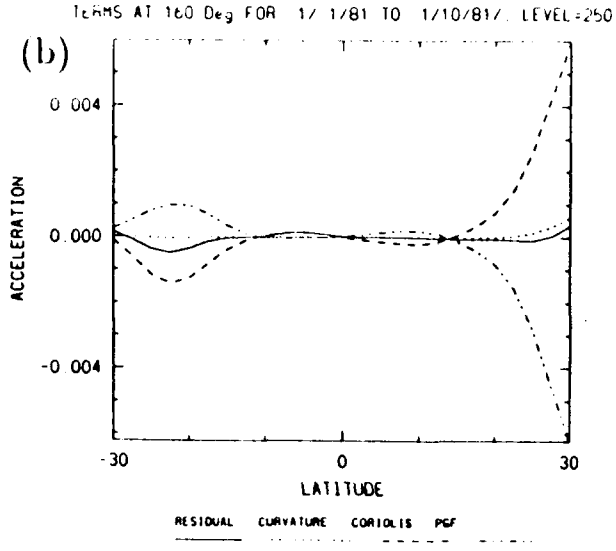
(b)
TERMS AT 160 Deg FOR 1/ 1/81 TO 1/10/81/ LEVEL=250
0 004
0 000
-0 004
ACCELERATION
-30
0
30
LATITUDE
RESIDUAL CURVATURE CORIOLIS PGF

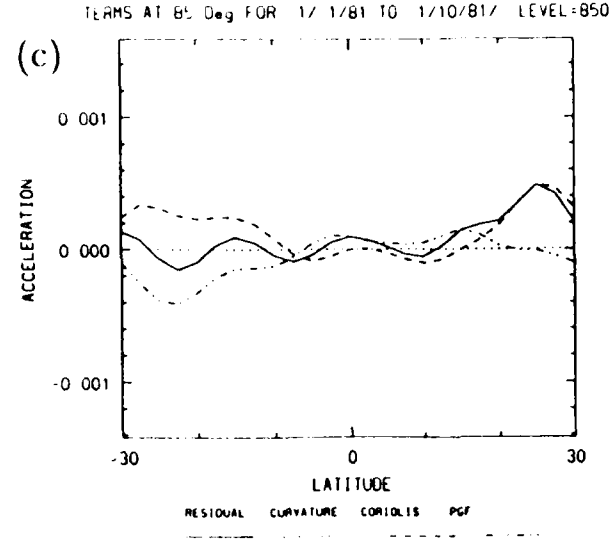
(c)
TERMS AT 85 Deg FOR 1/ 1/81 TO 1/10/81/ LEVEL=850
0 001
0 000
-0 001
ACCELERATION
-30
0
30
LATITUDE
RESIDUAL CURVATURE CORIOLIS PGF

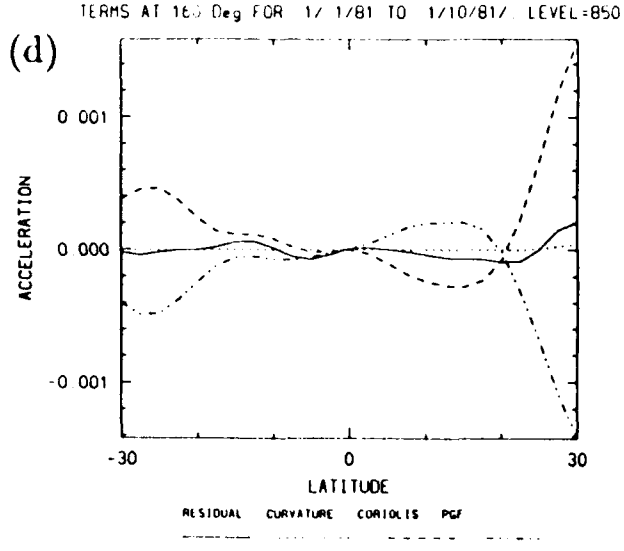
(d)
TERMS AT 160 Deg FOR 1/ 1/81 TO 1/10/81/ LEVEL=850
0 001
0 000
-0 001
ACCELERATION
-30
0
30
LATITUDE
RESIDUAL CURVATURE CORIOLIS PGF

Figure 4.10: Thirty day average of ratio between the residual term and largest term in Eq. (4.1) for January 1981. (a) 85 degrees east and 250 mb, (b) 85 degrees east and 850 mb, (c) basin ratio at 250 mb, and (d) basin ratio at 850 mb.

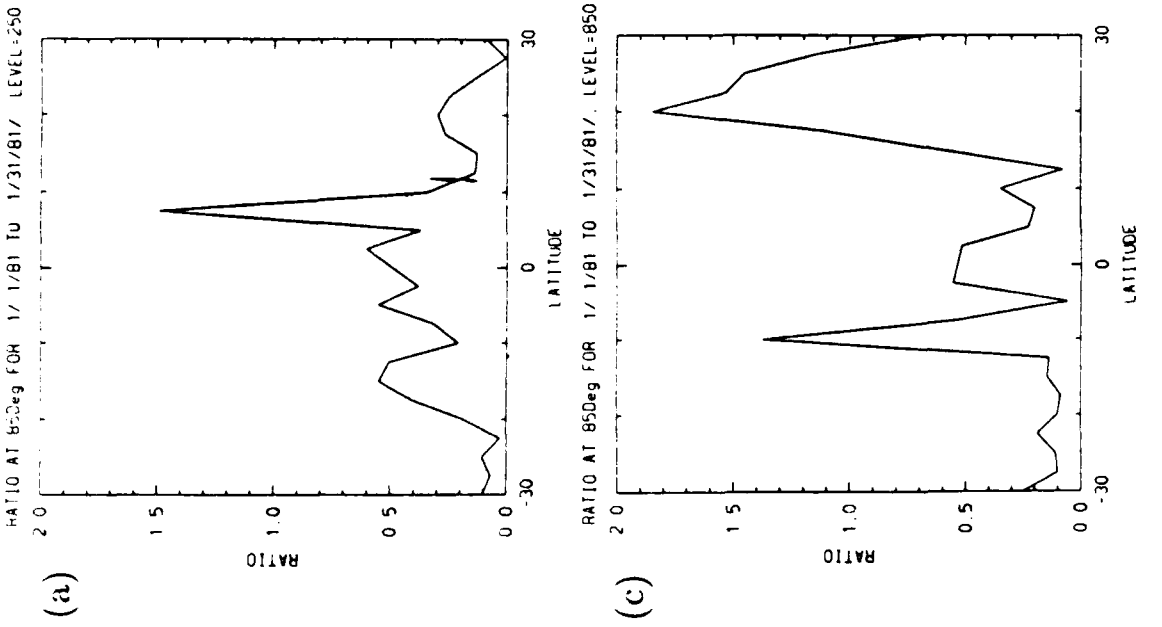
(a)
RATIO AT 850eg FOR 1/ 1/81 TO 1/31/81/ LEVEL=250
RATIO
LATITUDE
(b)
BASIN RATIO FOR 1/ 1/81 TO 1/31/81/ LEVEL=250
RATIO
LATITUDE
(c)
RATIO AT 850eg FOR 1/ 1/81 TO 1/31/81/. LEVEL=850
RATIO
LATITUDE
(d)
BASIN RATIO FOR 1/ 1/81 TO 1/31/81/. LEVEL=850
RATIO
LATITUDE

in figure 4.10a is the large spike around 8 degrees north. When compared to the same area in Fig. 4.8, this area is where all of the terms in Eq. (4.3) are quite small. In this region the pressure gradient and Coriolis forces are of the same sign, so that they add to give a residual that is larger than any other term. It is difficult to interpret the accuracy of the quasi-balanced approximation in this region. Given that the neglected residual is the largest term, it would appear that the flow is unbalanced. Figure 4.10b shows a similar feature at 10 degrees south which may be due to inflow into the ITCZ.

More general conclusion can be reached by examaning the basin ratio since any large amplitude ratio value can be assumed to be representative of the larger area. Figure 4.10c shows this basin ratio at 250 mb for the month of January 1981. Between 10 degrees south and the equator, the ratio varies between .4 and .9. This is the area of the ITCZ where strong convection results in divergence at 250 mb and convergence at 850 mb. This divergence/convergence pattern would have associated meridional accelerations. The strong inflow-induced residual is evident on Fig. 4.10d, where the residual is nearly 1.4 times larger than the next largest term. Attention should be paid to the areas south of the obvious ITCZ. Here, the ratio is much smaller. Thus, the quasi-balanced approximation appears to work well for flow outside of convectively dominated areas. That the quasi-balanced approximation doesn't appear to work well in areas of strong convection (with convergent areas of flow) is not surprising. The limiting factor may be the absence of the cumulus friction processes. These processes tend to act as a balance to divergence. The inclusion of these physics should make for a more valid approximation.

4.3 El Nino Southern Oscillation

If the preceeding figures can be thought of as representing the avera e state of the tropical atmosphere during a one month period, then the strong ENSO event of 1982–1983 can be considered as a strong deviation from this average. With the conclusion about the validity of the quasi-balanced approximation in areas of strong convection in mind, the same types of figures will now be presented for January 1983, near the peak of this particular ENSO event (Gill and Rasmussen 1983). What differences should be

expected? In the Australian monsoon area (the 'basin' region), convection should be weaker, and with all other things being equal, the quasi-balanced approximation might prove to be more accurate. The opposite is true in the central Pacific, where the convection has increased. Figure 4.11 should be compared to Fig. 4.3. While some subtle differences do exist, such as the lessening of the residual over the Australian land mass and Indonesia, the two figures are remarkably similar. It is possible that the data is not dense enough to show the difference, or that the time averaging scheme has smoothed the difference.

Figure 4.12, the terms at 850 mb, shows some differences. Both the Coriolis and pressure gradient forces are smaller in magnitude in the Australian area which result from the weakened circulation during the ENSO event.

Figure 4.13 presents the 10 day average. When compared to Fig. 4.5, the non-ENSO period at 250 mb, few differences are evident. Figure 4.14, at 850 mb, does show some differences from the non-ENSO period. Looking at the curvature term, the non-ENSO figure (4.6) has values less than $10^{-5}\ ms^{-2}$ over most of the western pacific, whereas the ENSO figure (4.14) shows values that are 4–5 times as large. This could be a result of the increased convection in this area of the Pacific.

Turning now to the cross sections, Figs. 4.15 a–d show the January averages for 1983. When Fig. 4.15a is compared to Fig. 4.8a, the residual is nearly the same except in the area near 20 degrees north. Reduced southern hemisphere convection causes a weaker Hadley cell, and thus the subtropical jet in this area would be weakened, resulting in a smaller residual term. Whether the quasi-balanced approximation is actually better will be seen in the ratio calculations. Figure 4.15b shows a general balance in the areas of greatest flow, but again it is difficult to interpret what is happening in the deep tropics. Figures 4.15 c–d show the 850 mb terms. As before in Figs. 4.8 c–d, the residual term has a much greater relative amplitude compared to the amplitude at 250 mb. It appears, at least from this figure, that the quasi-balanced approximation is more valid in the upper atmosphere than in the lower levels. Since the residual includes not only meridional accelerations but frictional effects, this should not be too surprising.

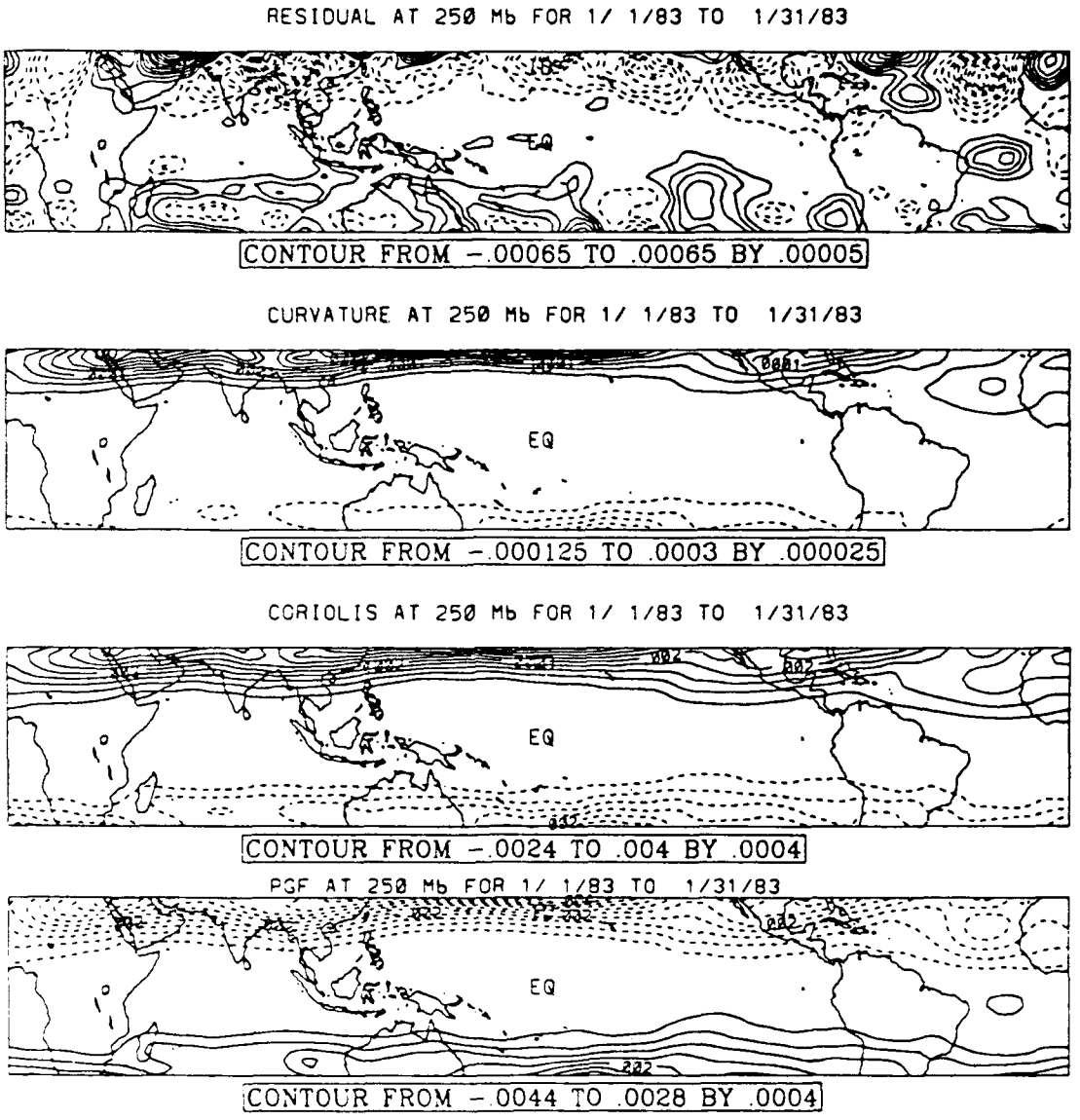

Figure 4.11: Thirty day average from January 1983, at 250 mb, plot of terms of Eq. (4.1). Units are ms^{-1}.

Figure 4.12: As in Fig. 4.11 except for 850 mb.

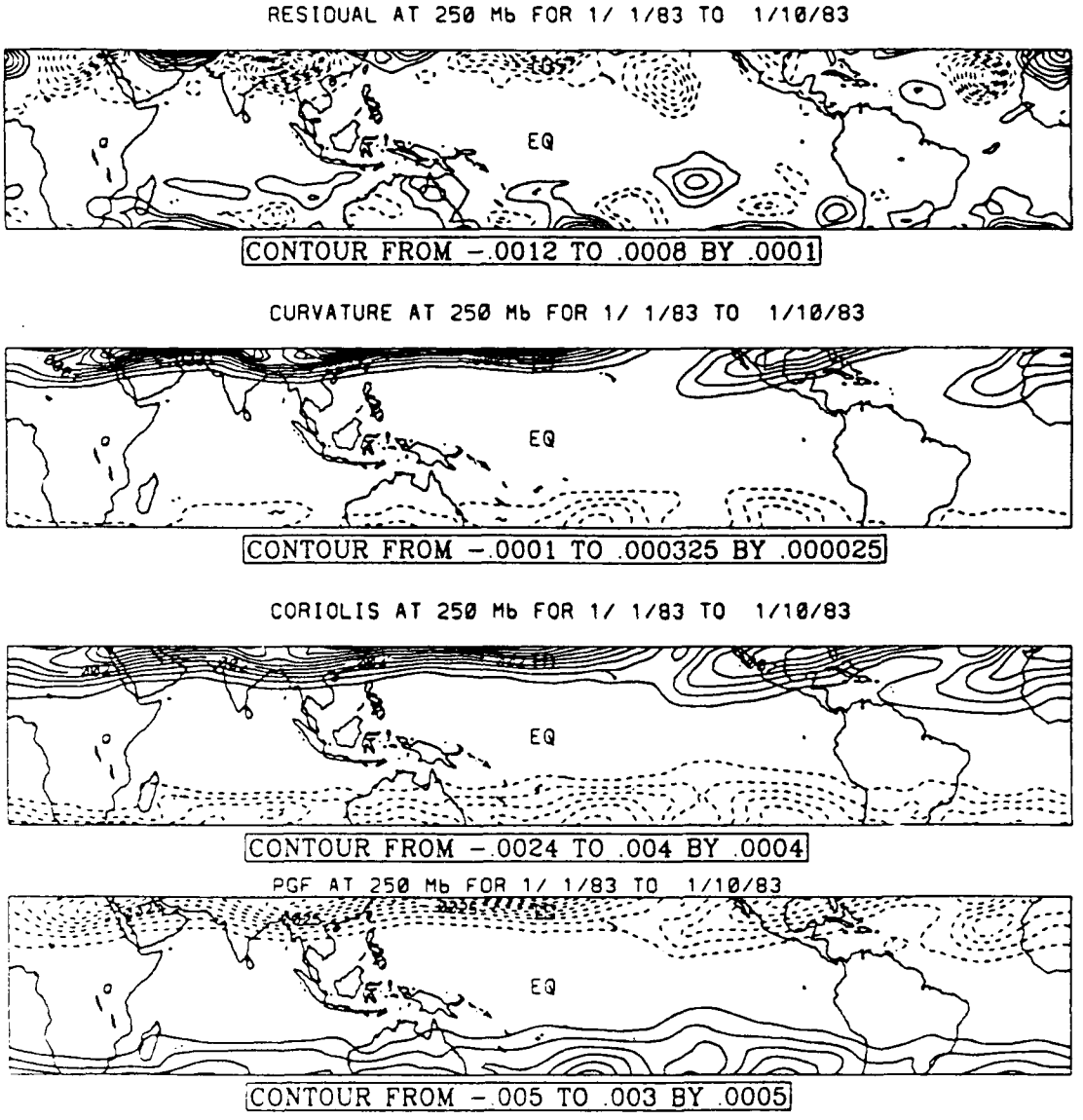

Figure 4.13: As in Fig. 4.12 except for 10 day average at 250 mb.

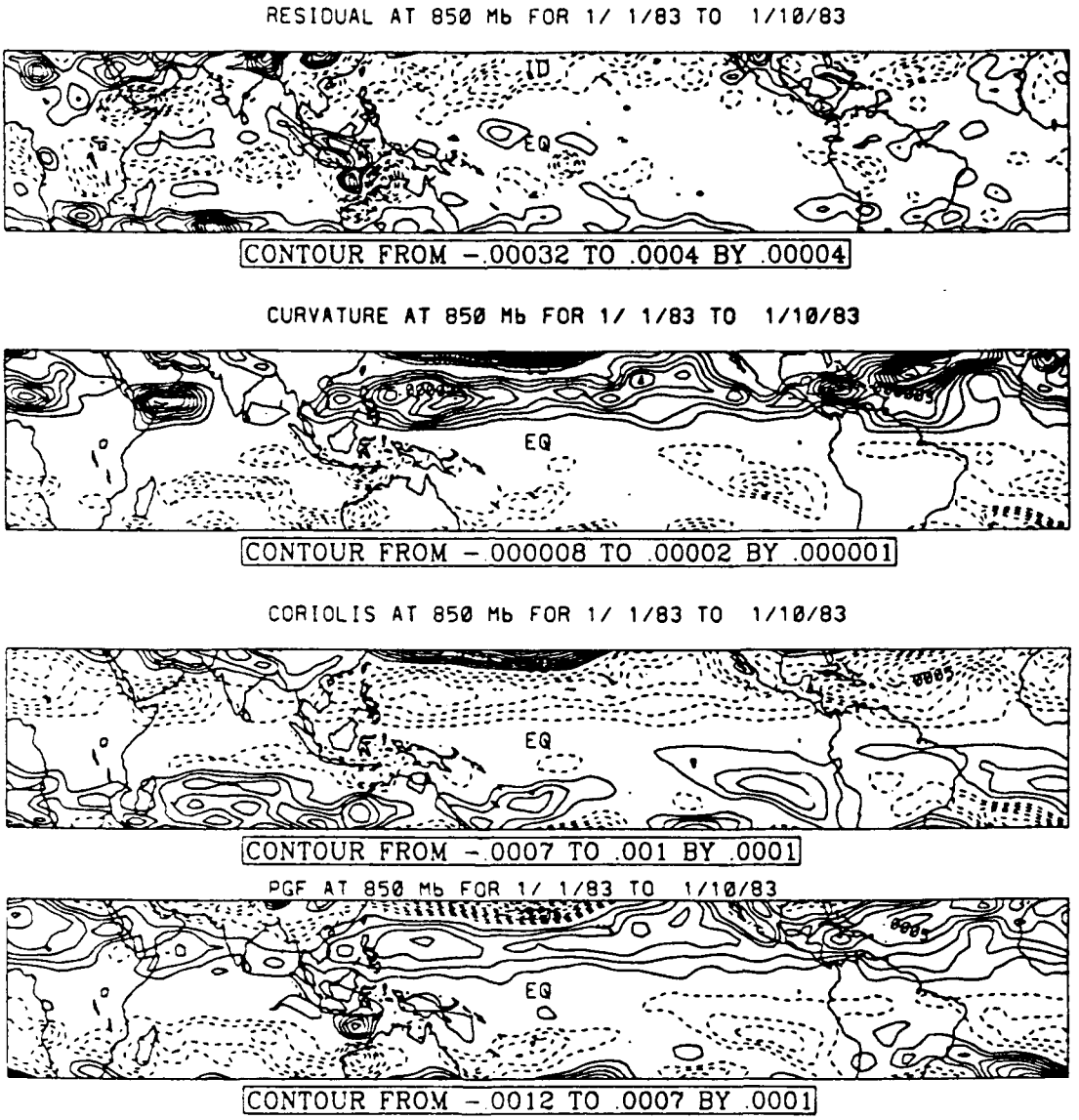

Figure 4.14: As in Fig. 4.13 except for 850 mb.

Figure 4.15: Thirty day averaged cross section of individual terms for January 1983 at (a) 85 degrees east and 250 mb, (b) 160 degrees east and 250 mb, (c) 85 degrees east and 850 mb, and (d) 160 degrees east and 850 mb.

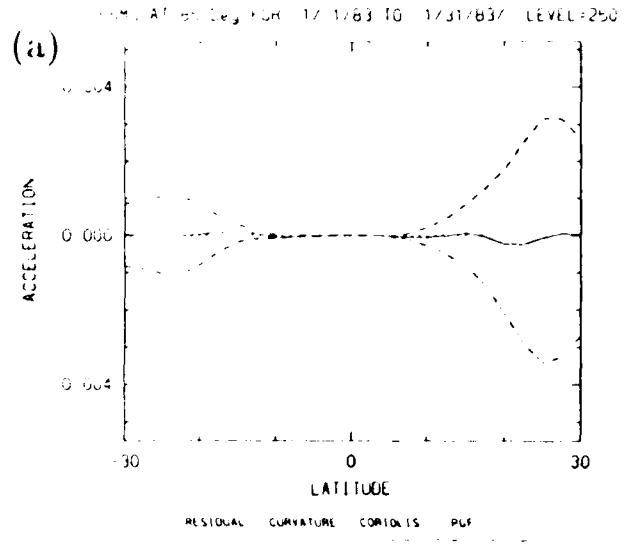
(a)
ACCELERATION
0 000
-0 004
-30
0
30
LATITUDE
RESIDUAL CURVATURE CORIOLIS PGF

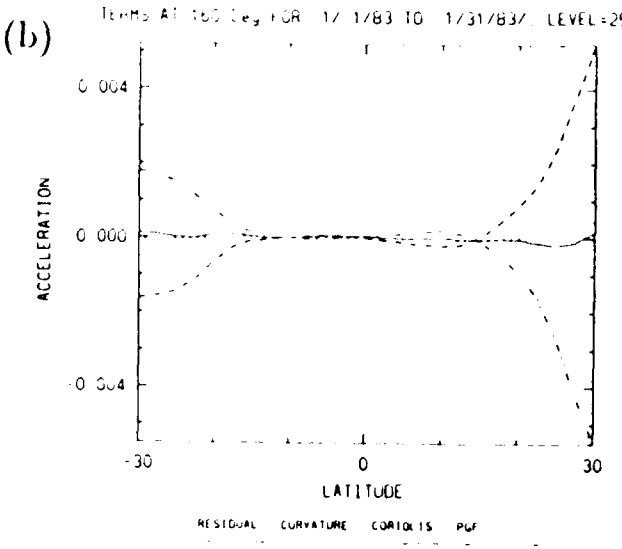
(b)
TERMS AT 160 Deg FOR 1/ 1/83 TO 1/31/83/ LEVEL=250
0 004
ACCELERATION
0 000
-0 004
-30
0
30
LATITUDE
RESIDUAL CURVATURE CORIOLIS PGF

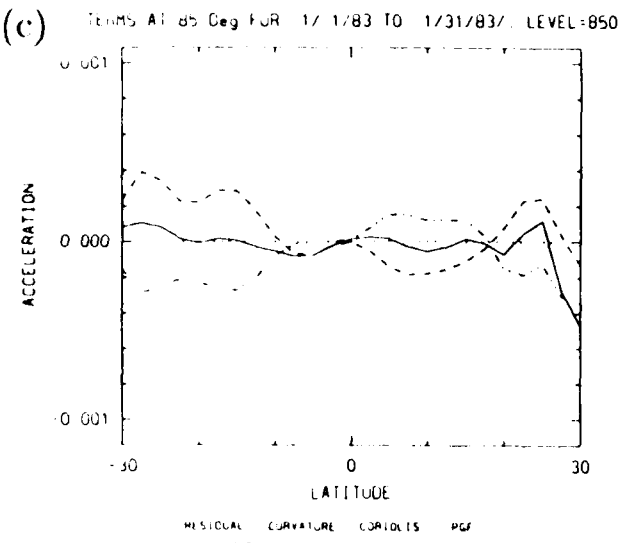
(c)
TERMS AT 85 Deg FOR 1/ 1/83 TO 1/31/83/ LEVEL=850
0 001
ACCELERATION
0 000
-0 001
-30
0
30
LATITUDE
RESIDUAL CURVATURE CORIOLIS PGF

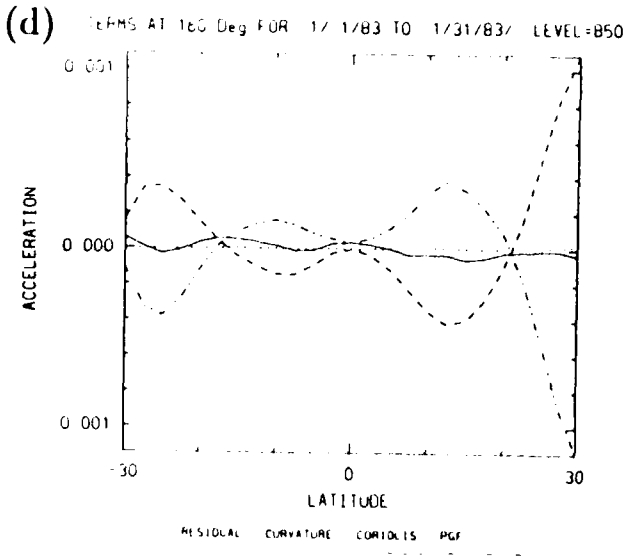
(d)
TERMS AT 160 Deg FOR 1/ 1/83 TO 1/31/83/ LEVEL=850
0 001
ACCELERATION
0 000
0 001
-30
0
30
LATITUDE
RESIDUAL CURVATURE CORIOLIS PGF

Figure 4.16: As in Fig. 4.15 except for 10 day average from January 1983, (a) 85 degrees east and 250 mb, (b) 160 degrees east and 250 mb, (c) 85 degrees east and 850 mb and (d) 160 degrees and 850 mb.

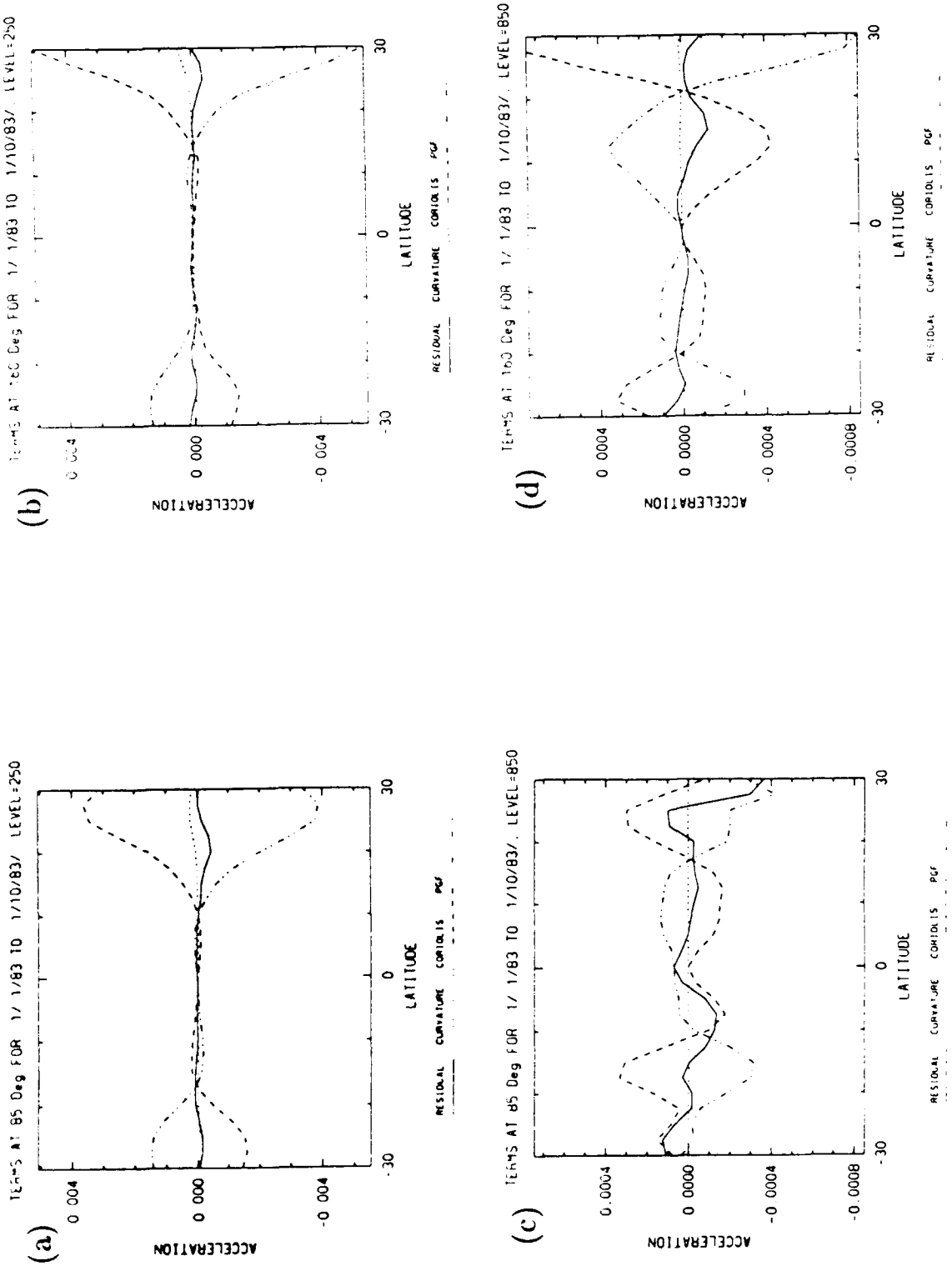
(a)
TERMS AT 85 Deg FOR 1/ 1/83 TO 1/10/83/ LEVEL=250
ACCELERATION
0.004
0.000
-0.004
LATITUDE
30
0
-30
RESIDUAL CURVATURE CORIOLIS PGF
(b)
TERMS AT 85 Deg FOR 1/ 1/83 TO 1/10/83/ LEVEL=250
ACCELERATION
0.004
0.000
-0.004
LATITUDE
30
0
-30
RESIDUAL CURVATURE CORIOLIS PGF
(c)
TERMS AT 85 Deg FOR 1/ 1/83 TO 1/10/83/ LEVEL=850
ACCELERATION
0.0004
0.0000
-0.0004
-0.0008
LATITUDE
30
0
-30
RESIDUAL CURVATURE CORIOLIS PGF
(d)
TERMS AT 85 Deg FOR 1/ 1/83 TO 1/10/83/ LEVEL=850
ACCELERATION
0.0004
0.0000
-0.0004
-0.0008
LATITUDE
30
0
-30
RESIDUAL CURVATURE CORIOLIS PGF

Figure 4.16 a–d shows 10 day average cross sections. These are very similar to the non-ENSO figures (4.9 a–d), but some differences are visible at 850 mb. Figure 4.16d shows a more fluctuating pattern of term sizes than does Fig. 4.9d, but the residual is still quite small in both figures. Even with the large changes in the convective forcing due to the ENSO signal, the quasi-balanced approximation appears to be valid. Although certain areas in Fig. 4.16d show that the approximation is not uniformly correct, such as at both 20 degrees north and south, the approximation of relative balance appears to hold fairly well.

Finally, Figs. 4.17 a–d shows the ratio calculations for January 1983. Particular attention should be given to Fig. 4.17d. Comparing 4.17d to 4.10d, a significant difference in the southern hemisphere is noted. In this basin area, the convection should lesson dramatically during a strong ENSO event. Figure 4.17d captures this change and shows that the quasi-balanced approximation again does better in areas of less convection. While convection is nearly always occurring in the tropics, it usually is confined to certain areas. There should also be large, convective free areas. These areas should be ideal for the quasi-balanced approximation. Note on nearly all of the ratio plots presented, specifically at 250 mb, the ratio in the subtropical areas is quite small. In this area, where the flow is not entirely quasi-geostrophic or convectivley driven, the quasi-balanced approximation does quite well.

While the quasi-balanced system was advertised as a possible basis for prediction in the tropics by Stevens *et al.* (1990), there are areas where the quasi-balanced approximation is poor. The potential vorticity equation obtained by making the approximation was shown to be quite capable of resolving the structure of this important variable. If the Hoskins *et al.* view of "potential vorticity thinking" is to be adopted, then this quasi-balanced approximation may be a way to combine the middle latitude and tropical areas into one dynamical scheme.

The analysis presented here suggests that the quasi-balanced approximation should be used selectly. For example, the approximation doesn't work well for areas of the atmosphere dominated by convection. While this is unfortunate, the approximation was

never advertised as being able to analyze and/or predict tropical motions on the spatial and/or temporal scale of individual convective elements. The inclusion of cumulus friction should also serve to improve the approximation. It is also interesting that the potential vorticity calculations obtained using the approximation form of Eq. (4.1) are quite similar to the full form calculation. The area of interest is an area of intense convection, and this convection causes the potential vorticity gradients to form. So while the quasi-balanced approximation doesn't work well for convectively dominated flow, potential vorticity, calculated in an area of continuous convection using the approximated potential vorticity equation, does appear to be resolved. The main point here is that convective flow is not described well, but the results of this convection can be approximated. Indeed, Stevens *et al.* (1990) have suggested that this approximation is useful for studying large, slowly evolving features in the tropical atmosphere. The small end of the scale may include disturbances as small as easterly waves. The approximation is good, both mathematically and physically, at describing what it is intended for. Any use of the quasi-balanced approximation as a predictive scheme would either have to limit the scale of predicted motions, or use a different scheme to predict the smaller scale, convective motions and then 'combine' the answers.

A logical extension of this study would be a spectral-based analysis of the approximation. Such an analysis would yield information as a function of zonal wavenumber. If a limiting wavenumber was found for validity, this would give more information than 'convective vs. bigger than convective' scales. With this approach, even features that are small in physical space, but dominated by long wavelength, such as the tropical cyclone outflow region, may be well described by the quasi-balanced approximation.

Figure 4.17: Thirty day average of ratio between the residual term and largest term in Eq. (4.1) for January 1983, (a) 85 degrees east and 250 mb, (b) 85 degrees east and 850 mb, (c) basin ratio at 250 mb and (d) basin ratio at 850 mb.

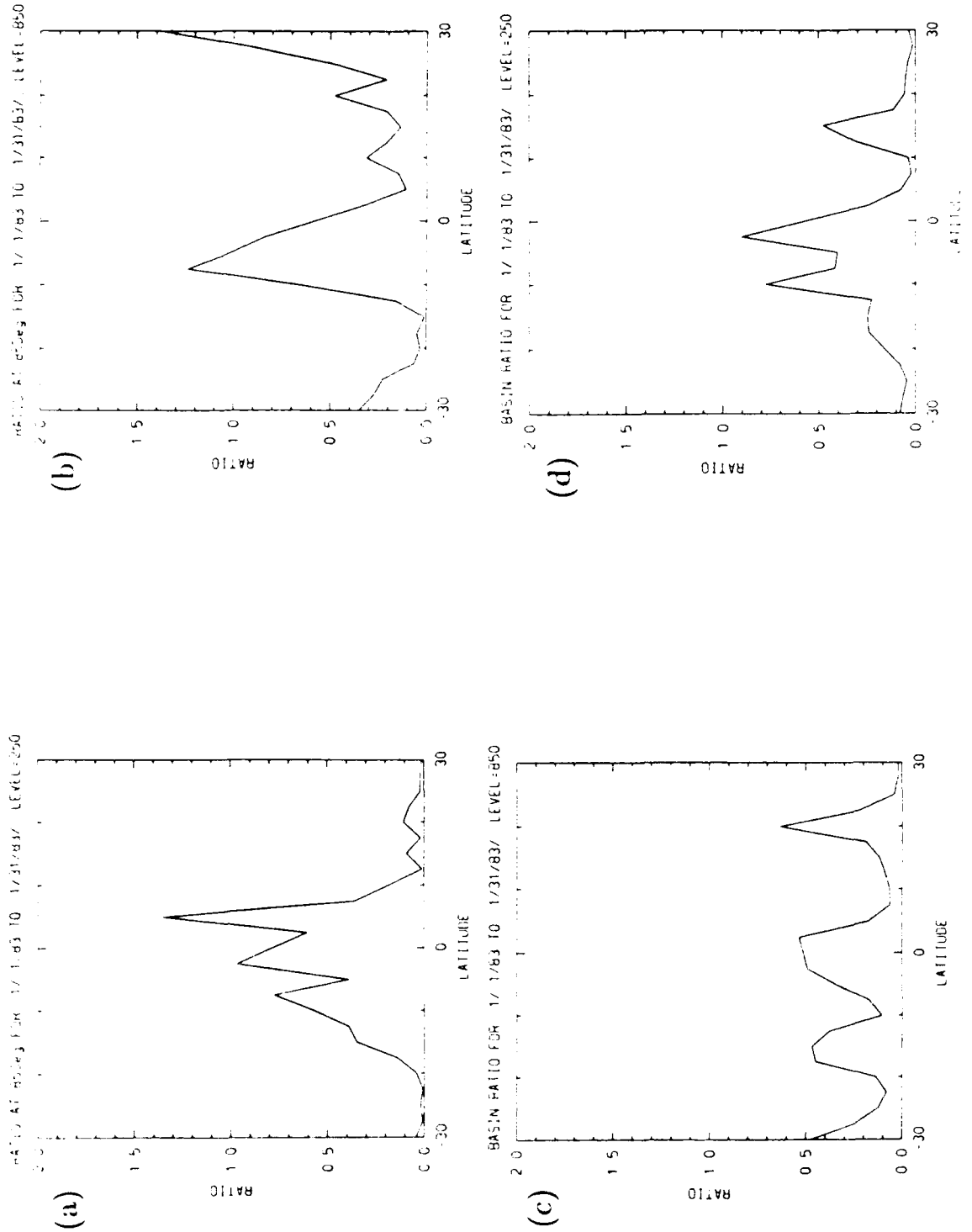
(a)
(b)
(c)
(d)
RATIO
LATITUDE
BASIN RATIO FOR 1/ 1/83 TO 1/31/83/ LEVEL=250
BASIN RATIO FOR 1/ 1/83 TO 1/31/83/ LEVEL=850

Chapter 5

SUMMARY AND CONCLUSIONS

In this thesis, isentropic potential vorticity is discussed and calculated with respect to the quasi-balanced approximation of Stevens *et al.* (1990). While not being a predictive scheme for tropical motions, the quasi-balanced approximation is the next step in the evolution of such a method. This approximation, which is a generalization of one put forth by Gill (1980), is based on the assumption of relative smallness of the meridional acceleration term in the meridional momentum equation. An important point is the inclusion of this meridional acceleration in the divergence equation, thus allowing for Kelvin waves in the solutions. These Kelvin waves are important in both establishing the tropical easterly wind field in the lower levels of the eastern Pacific Ocean, and the QBO of the equatorial stratosphere.

Calculations were made of isentropic potential vorticity for a period that corresponded to Phase II of AMEX. These calculations, undertaken because of the stress placed on potential vorticity in tropical balance models, showed many interesting features. Among these were the presence of an area of reversed pole-to-equator potential vorticity gradient. This area of reversed gradient was an interesting discovery, as it was very similar to another area of reversed gradient found by Burpee (1972) over Africa. While the African region of potential vorticity was thought to exist because of the reversed temperature gradient in the Sahara Desert, the discovery of a similar area in Australia lends doubt to this theory. It is now believed that convective forcing alone can cause gradient reversals of the magnitude seen, both in Africa and Australia.

The data fields for this Phase II AMEX period were looked at for two periods. The first, defined as an active monsoon period by Gunn *et al.* (1989), shows an area of

reversed potential vorticity gradient to be present. The second time period, defined to be an inactive period, or monsoon break, shows that not only have the low level flows (both easterlies and westerlies) decreased, so has the potential vorticity field. This is strong support that the anomaly is caused by convective forcing. Whether the convection or the potential vorticity gradient weakened first can not be deduced from this study. Schubert *et al.* (1991) suggest that the potential vorticity anomalies may become so large from the convective forcing that the strong area of convection may be destroyed by the instability that the convection creates. That this organized convection carries the seed of its own destruction may lead one to believe that this may be a factor in these monsoon breaks.

The quasi-balanced approximation was tested in several different ways. First, fields using the quasi-balanced form of the potential vorticity equation were compared to the same fields calculated with the 'full' equation. The results agreed very well. This suggests that the quasi-balanced approximation is quite good at calculating this important variable.

The second test of the approximation involved a calculation of terms of the equation, and the equality was tested. Individual terms were presented that showed the flow in the subtropics was dominating the tropical area. When cross sections of individual terms were presented, it was obvious that the residual term was small in these subtropical areas of stronger flow. The situation near the equator was not as clear, however. To view the relative importance of the neglected residual term, a ratio was defined . The smaller the ratio, the better the approximation. What was evident from the ratio plots was that the approximation has some weaknesses in areas of strong convection. These areas, with their associated convergence/divergence patterns, did not appear to be described well with the quasi-balanced approximation.

While this is unfortunate, this does not mean that the approximation should not be pursued. What is needed is a test of the approximation, not on gridpoint data, but on data that has been analyzed in spectral space. This will allow the test to be done on certain length scales of flows. It is hypothesized that the approximation will well describe features of moderate to long wavelength, possibly even, as suggested by Stevens *et al.* (1990), down to the scale of tropical easterly waves. More likely though, the

quasi-balanced approximation will be found to be useful for describing (and hopefully, predicting) tropical climate dynamics.

In summary, then, the importance of potential vorticity was verified for use as a tracer in describing tropical motions, and the ability of convection alone to form anomalous areas of potential vorticity was established. The tests of the validity of the quasi-balanced approximation were somewhat inconclusive. It was shown that the approximation worked well in non-convective areas. The validity of the approximations appears suspect in convectively dominated areas, but the approximation should really be tested with respect to wavelength of disturbances, a test not performed in this paper.

REFERENCES

Burpee, R.W., 1972: The origin and structure of easterly waves in the lower troposphere of North Africa. *J. Atmos. Sci.*, **29**, 77-90.

Burpee, R.W., 1974: Characteristics of North African easterly waves during the summers of 1968 and 1969. *J. Atmos. Sci.*, **31**, 1556-1570.

Charney, J.G. and M.E. Stern, 1962: On the stability of internal baroclinic jets in a rotating atmosphere. *J. Atmos. Sci.*, **19**, 159-172.

Davidson, N.E., 1984: Short term fluctuations in the Australian monsoon during winter MOMEX. *Mon. Wea. Rev.*, **112**, 1697-1708.

Ertel, H., 1942: Ein neuer hydrodynamischer Wirbelsätz. Meteorologische Zeitschrift, Vol 59, No. 9, page 22.

Frank, N.L., 1970: Atlantic tropical systems of 1969. *Mon. Wea. Rev.*, **98**, 307-314.

Frank, W.M. and J.L. McBride, 1989: The vertical distribution of heating in AMEX and GATE cloud clusters. *J. Atmos. Sci.*, vol46 3464-3478.

Gill, A.E., 1980: Some simple solutions for heat-induced tropical circulation. *Quart. J. R. Met. Soc.*, **06**, 447-462.

Gill, A.E., and E.M. Rasmusson, 1983: The 1982-1983 climate anomaly in the equatorial Pacific. *Nature*, **306**, 229-234.

Gunn, B.W., J.L. McBride, G.J. Holland, T.D. Keenan, N.D. Davidson, and H.H. Hendon, 1989: The Australian summer monsoon circulation during AMEX phase II. *Mon. Wea. Rev.*, **117**, 2554-2574.

Hack, J.J., W.H. Schubert, D.E. Stevens, and H.-C. Kuo, 1989: Response of the Hadley circulation to convective forcing in the ITCZ. *J. Atmos. Sci.*, **46**, 2957-2973.

Hoskins, B.J., M.E. McIntyre, and D.W. Robertson, 1985: On the use and significance of isentropic potential vorticity maps. *Quart. J. Roy. Met. Soc.*, **111**, 877-946.

Matsuno, T., 1966: Quasi-geostrophic motions in the equatorial area. *J. Meteor. Soc. Japan*, **44**, 25-43.

McBride, J.L. and G.J. Holland, 1989: The Australian monsoon experiment (AMEX): early results. *Aus. Met. Mag.*, **37**, 23-35.

Moura, A.D., 1976: The eigensolutions of the linearized balance equations over a sphere. *J. Atmos. Sci.*, **33**, 877-907.

Schubert, W.H., P.C. Ciesielski, D.E. Stevens, and H.-C. Kuo, 1991: The evolution of potential vorticity in the Hadley circulation. *J. Atmos. Sci.*, **48**, in press.

Stevens, D.E. and P.E. Ciesielski, 1986: Inertial instability of horizontally sheared flow away from the equator. *J. Atmos. Sci.*, **43**, 2845-2856.

Stevens, D.E., P.E. Ciesielski, H.-C. Kuo, W.H. Schubert, and P.E. Ciesielski, 1990: Quasi-balanced dynamics in the tropics. *J. Atmos. Sci.*, **47**, 2262-2273.

Wallace, J.M. and V.E. Kousky, 1968: Observational evidence of Kelvin waves in the tropical stratosphere. *J. Atmos. Sci.*, **25**,, 900-907.

Wallace, J.M, 1983: The climatological mean stationary waves: Observational evidence. *Large-scale Dynamical Processes in the Atmosphere*, B.J. Hoskins, R.P. Pearce, Eds., Academic Press, 27-53.

Yanai, M.S., Esbensen, and J.H. Chu, 1973: Determination of bulk properties of tropical cloud clusters from large-scale heat and moisture budgets.*J. Atmos. Sci.*, **30**, 611-627.